Tectonophysics 635 (2014) 6–32

Contents lists available at ScienceDirect

Tectonophysics

journal homepage: www.elsevier.com/locate/tecto

Late Cretaceous to Late Eocene Hekimhan Basin (Central Eastern Turkey) as a supra-ophiolite sedimentary/magmatic basin related to the later stages of closure of Neotethys

Matthew G. Booth [a,*], Alastair H.F. Robertson [a], Kemal Tasli [b], Nurdan İnan [b]

[a] The Grant Institute, School of GeoSciences, University of Edinburgh, West Mains Road, Edinburgh EH9 3JW, United Kingdom
[b] Department of Geology, Mersin University, Mersin 33343, Turkey

ARTICLE INFO

Article history:
Received 7 August 2013
Received in revised form 30 April 2014
Accepted 30 May 2014
Available online 6 June 2014

Keywords:
Supra-ophiolite basin
Late Cretaceous–Late Eocene
Turkey
Neotethys

ABSTRACT

The Hekimhan Basin is here put forward as a type example of a globally important class of basin, known as a supra-ophiolite basin. Such basins form after the emplacement of ophiolitic (i.e. oceanic) rocks onto a passive continental margin, but long prior to continental collision. The Hekimhan Basin developed as part of the northern margin of the Tauride microcontinent during the collision and suturing of two Neotethyan oceans to the north, namely the Inner Tauride Ocean and the İzmir–Ankara–Erzincan ocean. The basin records two main stages of tectonic development, during latest Cretaceous to Late Eocene time. The first phase of basin development during the Late Cretaceous (Maastrichtian) began with the erosion of emplaced ophiolitic rocks, resulting in non-marine clastic sedimentation. Subsequently, the basin rapidly subsided, in response to inferred regional crustal extension, resulting in the deposition of hemipelagic marls and local sapropelic mudstones. The axial parts of the basin experienced alkaline, within-plate-type, basaltic volcanism. The Late Maastrichtian culminated in deposition of shallow-marine carbonates. Overlying Paleocene sediments are restricted to thin, localised, marine evaporates, associated with a low-angle unconformity. The second stage of basin development began during the Early Eocene with deposition of shallow-marine carbonates, coupled with localised basaltic volcanism, again of extensional type. The basin emerged during the Mid–Late Eocene in a late-stage collisional to post-collisional setting. Compressional deformation largely reflects post-suture tightening. A short-lived marine transgression occurred during the Mid-Miocene. The basin was later deformed by both left-lateral and right-lateral strike-slip.
Several different tectonic models are considered, notably extension related to the northward pull of a still-subducting oceanic slab, and back-arc extension related to northward subduction of Neotethys (to the south). The first alternative is consistent with the development of adjacent supra-ophiolite basins (e.g. Ülükışla and Darende Basins), and also with supra-ophiolite basins elsewhere (e.g. SE Turkey; Balkans; Oman).

1. Introduction

Many types of sedimentary basin are nowadays quite well understood (e.g. rift basins, foreland basins, and strike-slip pull-part basins) such that current research commonly focuses on modelling of the driving mechanisms (e.g. processes of subsidence). However, some sedimentary and volcanic basins have tended to be treated as once-offs without realising that they represent general types of basin in a global perspective. Chief amongst these are supra-ophiolite basins. These are basins associated with thick sedimentary and/or magmatic rocks that have developed on top of emplaced ophiolitic rocks. Ophiolites are generally accepted as fragments of oceanic crust that have been tectonically emplaced, commonly onto adjacent passive margins. The emplacement typically takes place relatively early in an orogenic cycle which terminated millions of years later with the complete subduction of oceanic crust and the suturing of opposing continents. Here, we will present and interpret new evidence for the initiation and development of an excellent example of one such pre-collisional supra-ophiolite basin, namely the latest Cretaceous–Late Eocene Hekimhan Basin in central eastern Turkey (Fig. 1). This paper builds on a parallel study of a neighbouring supra-ophiolite basin, the Darende Basin (Booth et al., 2013).

We will first explain the regional tectonic setting, then present and interpret the geological development of the Hekimhan Basin as a series of time slices. We will emphasise the tectonic controls on basin formation, which are primarily extensional. The Hekimhan Basin is compared with several other supra-ophiolite basins in the region, elsewhere in Neotethys and in other orogenic belts. Because understanding of such supra-ophiolite basins is still limited, it is essential to fully document individual examples as case histories. Accordingly, we present an integrated account of the Hekimhan Basin including new sedimentological, geochemical,

* Corresponding author. Tel.: +44 7834827772.
E-mail address: Matthew_Booth3@hotmail.com (M.G. Booth).

http://dx.doi.org/10.1016/j.tecto.2014.05.039
0040-1951/

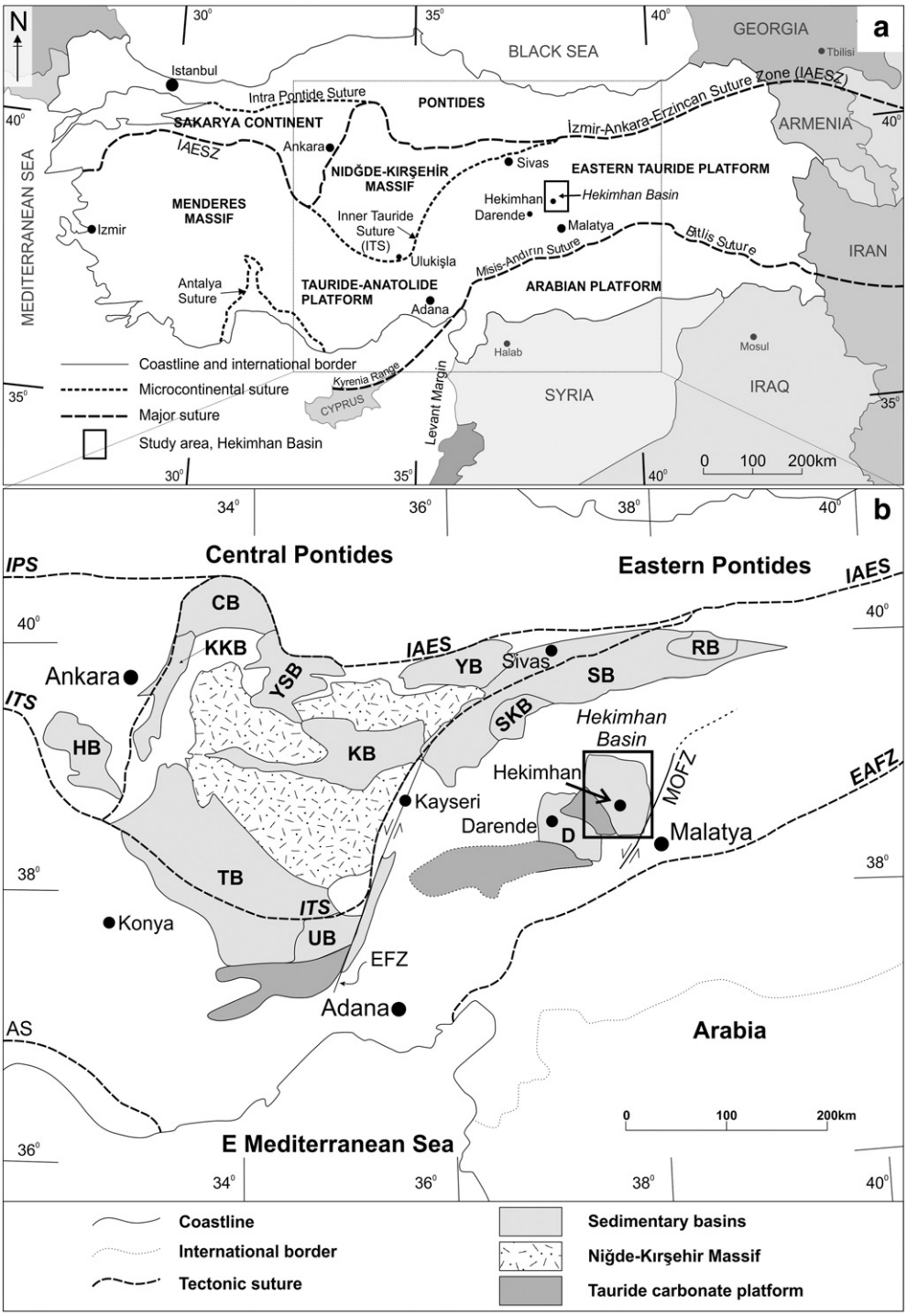

Fig. 1. Regional tectonic setting. (a) Outline tectonic map showing the location of the Hekimhan Basin in eastern Anatolia in relation to the suture zones (marked by box). (b) Outline tectonic map showing the main tectonic units of central Anatolia in relation to the Hekimhan Basin. Key to main structural features: IPS, Intra-Pontide Suture; ITS, Inner Tauride Suture; AS, Antalya Suture; IAES, İzmir–Ankara–Erzincan Suture; EAFZ, East Anatolian Fault Zone; MOFZ, Malatya–Ovacık Fault Zone; EFZ, Ecemiş Fault Zone. Key to major sedimentary basins: HB, Haymana Basin; KKB, Kırıkkale Basin; CB, Çankırı Basin; YSB, Yozgat-Sorgun Basin; KB, Kızılırmak Basin; YB, Yıldızeli Basin; SKB, Şarkışla Basin; SB, Sivas Basin; RB, Refahiye Basin; TB, Tuzgölü Basin; UB, Ulukışla Basin; D, Darende Basin. Main data sources: Görür et al. (1998) and Clark and Robertson (2002, 2005).

micropalaeontological and structural data, which we synthesise followed by discussion of several alternative tectonic models.

The time-scale used here is that of Gradstein et al. (2004).

2. Regional tectonic setting

The Hekimhan Basin (~1000 km^2) is located within the Tauride Mountains in central eastern Turkey ~80 km north of the city of Malatya (Fig. 1a). The setting of the Hekimhan Basin in relation to the suture zones making up Turkey is shown in Fig. 1b. The basin, as defined here, is made up of sedimentary and igneous rocks of latest Cretaceous (Maastrichtian) to Late Eocene age, although Mid-Miocene marine sediments are also locally present. The basin is directly floored by emplaced ophiolite-related (i.e. oceanic) material; hence, it is an example of a supra-ophiolite basin. Beneath, there is a Mesozoic carbonate platform unit of continental origin, which forms part of the regional-scale

Tauride–Anatolide continent extending across Turkey (Figs. 1 and 2). The ophiolitic rocks were emplaced southwards during Late Cretaceous time from an oceanic basin that was located to the north during the Mesozoic. To the west of the Hekimhan Basin is a continental unit known as the Niğde–Kırşehir Massif, or as the Central Anatolian Crystalline Complex (CACC), which consists primarily of Mesozoic metamorphic rocks (Figs. 1 and 2).

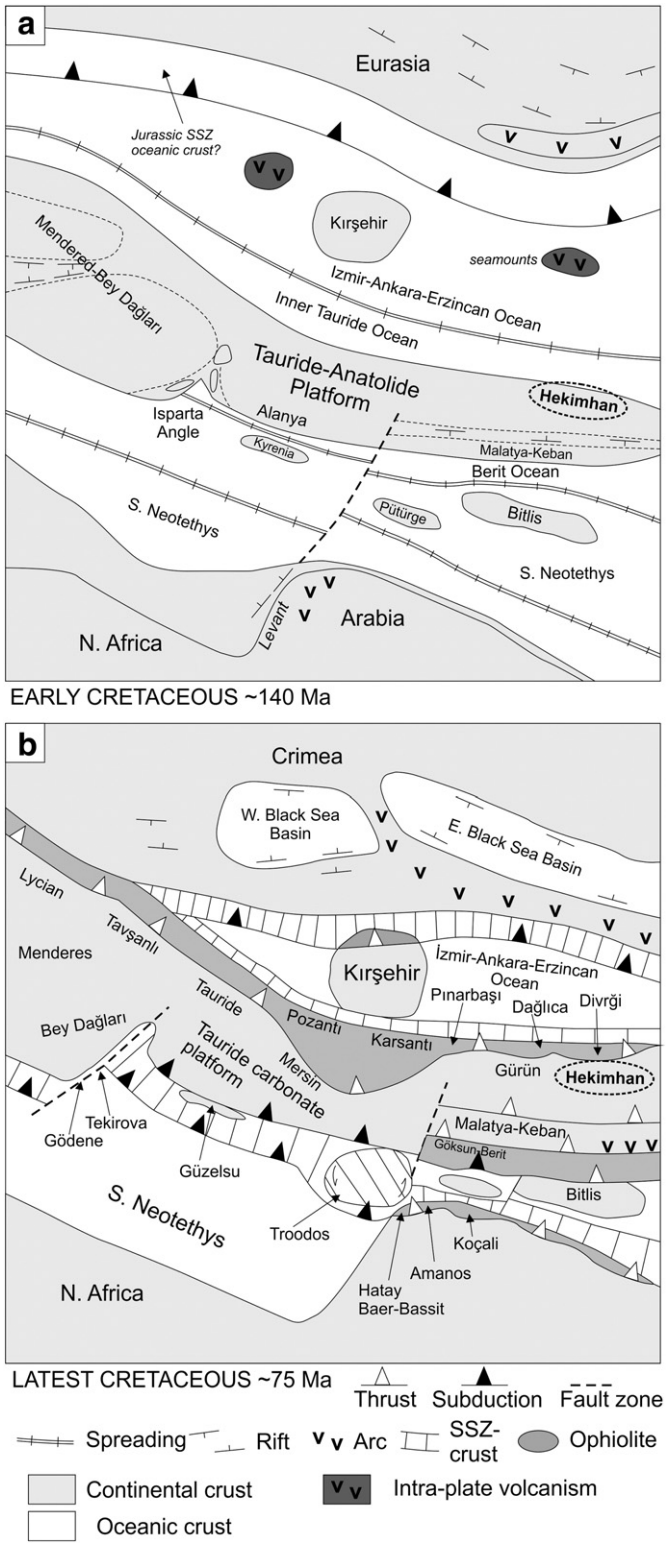

Fig. 2. Regional palaeotectonic reconstructions of the Eastern Mediterranean region. (a) Early Cretaceous. (b) Late Cretaceous (modified from Robertson et al., 2012). See text for explanation.

Neotethys was palaeogeographically complex and included several microcontinents of differing size and location (Fig. 2a and b). These are believed to have included the large Tauride–Anatolide continental unit and the smaller Niğde–Kırşehir microcontinent. The Niğde–Kırşehir Massif is widely considered to have rifted from the much larger Tauride–Anatolide continental unit, possibly during the early Mesozoic or even the Late Palaeozoic. This rifting is commonly interpreted to have created a small Mesozoic ocean basin known as the Inner Tauride Ocean (Görür and Tüysüz, 2001; Görür et al., 1984, 1998; Parlak et al., 2012, 2013a; Robertson et al., 2012, 2013a,b). One key line of evidence supporting the existence of the Inner Tauride Ocean is the occurrence of Late Cretaceous–Paleocene high pressure-low temperature (HP-LT) metamorphism affecting the northern margin of the Tauride–Anatolide carbonate platform (i.e. the Tavşanlı and Afyon zones; e.g. Okay et al., 2006; Robertson et al., 2009; Pourteau et al., 2010). The most easterly known equivalent of the HP-LT Anatolide metamorphic belt is located east of Kayseri (N of Pınarbaşı), about 150 km west of the Hekimhan Basin. It is possible that equivalents of the Anatolide HP-LT belt are present at depth beneath central eastern Anatolia but geophysical data (e.g. deep seismic data) would be needed to test this.

The Niğde–Kırşehir microcontinent is generally accepted to have been separated from the Pontides, part of the Eurasian continental margin, by an oceanic basin, known as the İzmir–Ankara–Erzincan Ocean (Okay and Tüysüz, 1999), or the Northern Neotethys (Şengör and Yılmaz, l981). In an alternative regional tectonic model, only one Mesozoic ocean basin existed, namely the İzmir–Ankara–Erzincan Ocean (e.g. Gürer and Aldanmaz, 2002). In this alternative model, ophiolitic rocks were emplaced southwards over both the Tauride–Anatolide and the Niğde–Kırşehir continental units (e.g. Floyd et al., 1991; 2000; Göncüoğlu et al., 1996–1997). However, in this paper we will assume the existence of a discrete Inner Tauride Ocean to the north of the Tauride–Anatolide carbonate platform in the study region. This ocean is likely to have closed in a diachronous manner such that it was largely or even entirely closed betweeen the Tauride–Anatolide continent and the Niğde–Kırşehir microcontinent during the latest Cretaceous (Fig. 2b), while both further east and further west the Inner Tauride Ocean is likely to have remained partially open until Late Palaeocene–Early Eocene time. The İzmir–Ankara–Erzincan ocean, further north finally closed by Mid-Eocene time (Okay and Şahintürk, l997; Sosson et al., 2010; Robertson et al., 2014).

The following aspects of the regional geology have a direct bearing on the Hekhiman Basin.

1. The ophiolitic rocks beneath the Hekhiman Basin and the adjacent areas were formed by spreading above a Late Cretaceous subudction zone, based on igneous petrological and geochemical evidence (Parlak et al., 2004, 2009, 2012, 2013a).
2. The ophioites in this region were emplaced, southwards onto the northern edge of the Tauride–Anatolide continent during latest Cretaceous time. The inferred driving mechanism was the collision of the subduction zone (above which the ophiolites formed) with the northerly, leading edge of the Tauride–Anatolide continent (Robertson et al., 2009).
3. The emplaced oceanic rocks in the region include a range of ophiolitic thrust sheets and accretionary mélange with both tectonic and sedimentary origins (Robertson et al., 2013b).
4. The latest Cretaceous regional ophiolite emplacement does not correspond to final closure of the Inner Tauride Ocean or the İzmir–Ankara–Erzican ocean; instead, suturing of these Neotetethyan basins was delayed until the Mid-Eocene (Okay and Şahintürk, 1997; Robertson et al., 2014).
5. To the south of the Hekhiman Basin was located a belt of Upper Cretaceous ophiolitic rocks, including the Göksun (N Berit), İspendere, Kömürhan and Guleman ophiolites. These ophiolites

formed in a supra-subduction setting (Parlak et al., 2009) within a Neotethyan basin, recently termed the Berit ocean (Karaoğlan et al., 2013; Robertson et al., 2012, 2013a). These ophiolites were finally emplaced (southwards) over a continental unit (or units) to the south known as the Pütürge and Bitlis massifs. The Bitlis massif experienced HP-LT metamorphism during the Late Cretaceous (Oberhänsli et al., 2010, 2014) related to the northward subdcuction. To the south of the Bitlis and Pütürge continental units was located a further oceanic basin, generally known as the southern Neotethys. This oceanic basin was not finally closed until Mid-Miocene time (Yılmaz, l993; Robertson et al., 2006, 2007; Okay et al., 2010).

6. The Hekimhan Basin developed during the latest Cretaceous in a pre-collisional setting, followed by its further development in a regional syn-collisional setting to post-collisional setting (Paleocene-Eocene). The first regional transgression of post-collisional sediments across much of Anatolia took place during the late Middle Eocene (Bartonian ~45 Ma) (Şengör and Yılmaz, l981).

2.1. Setting of the Hekimhan Basin

Supra-subduction zone ophiolite genesis and emplacement during the Late Cretaceous were necessary precursors to the formation of the Hekimhan Basin (Fig. 2b). The basin originated soon afterwards, still during latest Cretaceous time, floored by ophiolitic material that had recently been emplaced southwards over the Tauride continental margin.

Two main types of sedimentary basin developed during the latest Cretaceous–Early Cenozoic closure of Neotethyan basins, around and to the north of the Hekimhan Basin. First, there are regional-scale accretionary forearc-type basins and collision-related basins that are located in the Pontides, north and east of the Niğde–Kırşehir Massif, along the southern margin of Eurasia (Koçyiğit, 1991; Nairn et al., 2013; Robertson et al., 2014). Such subduction and collision-related basins (Görür et al., 1984) are not considered further here. Secondly, there are basins that developed on top of newly emplaced ophiolitic rocks, which are the subject of this paper. From west to east these are the Ülükışla Basin (Alpaslan et al., 2006; Clark and Robertson, 2002, 2005; Zorlu et al., 2011), the Şarkışla Basin, the Darende Basin (Booth et al., 2013; Gürbüz and Gül, 2005), the Hekimhan Basin and the southern part of the large Sivas Basin further north (Kavak et al., 1997; Yılmaz and Yılmaz, 2004; 2006; Poisson et al., 1996).

2.2. Previous work

The Hekimhan Basin was investigated by the Turkish General Directorate of Mineral Research and Exploration (MTA) during regional geological mapping of Turkey (~1936). However, the first comprehensive geological study was not completed until much later (Ayan, 1961). The first detailed stratigraphy of the Hekimhan Basin was by Gürer (1994). The Hekimhan Basin was found to host mineral resources (Yılmaz et al., 1993), including copper and gold-bearing iron-oxide deposits related to syenite intrusion and hydrothermal alteration (Kuşcu et al., 2011), also iron deposits (Stendal et al., 1995; Uçurum et al., 1996) and evaporites (Palmer et al., 2004; Yalçın and Bozkaya, 1996). The ore mineralogy and geochemistry of the ophiolitic rocks beneath the Hekimhan Basin were also reported (Marschik et al., 2008; Yalçin et al., 2009). Early palaeontological studies underpinned a basic stratigraphic nomenclature of the Hekimhan Basin (Özdemir and Tunç, 1993). This was followed by more specific studies of foraminifera and rudist bivalves (Çaglar and Önal, 2009). Little sedimentological work was carried out prior to this study, although there is some information on clay minerals (Yalçın and Bozkaya, 1995; Yalçın et al., 2009). Synthesising the then available geological information, Gürer (1994, l996) interpreted the Hekimhan Basin as a magmatically active back-arc basin. Recent studies include petrography and geochemistry of Cretaceous–Eocene alkaline intrusive rocks (Özgenç and İlbeyli, 2009) and the geochemistry and isotopic dating of Miocene volcanic rocks (Gürsoy et al., 2011; Kürüm et al., 2008).

3. Stratigraphic and structural framework

During this work a new geological map (Fig. 3) was prepared for the Hekimhan Basin by compiling and field checking existing information (e.g. Gürer l994; l996), coupled with the remapping of key stratigraphic and structural locations. Several cross-sections were prepared (Fig. 4a–c) to indicate the typical structural relationships.

Most of the Hekimhan Basin is exposed to the northwest of the regional NE–SW striking sinistral neotectonic Malatya–Ovacik fault zone. The southeastern part of the basin is cut and offset by this fault zone, which is also associated with a Plio-Quaternary sedimentary fill. The latest Cretaceous to Paleogene lithologies are underlain by ophiolite-related lithologies. Shallow-water carbonate rocks are exposed locally in the southwest of the basin, related to the regional Tauride carbonate platform. However, the contact between the carbonate platform and the basinal rocks is not exposed in the field area. Based on stratigraphic thickness variation, the basin depocentre is inferred to be located ~12 km northwest of Hekimhan town (Fig. 3).

The oldest sediments above the ophiolite-related lithologies and, where exposed, the underlying Mesozoic neritic carbonates are latest Cretaceous and shallow-marine in origin. A Paleocene-aged basin-wide low-angle (~5°) unconformity separates latest Cretaceous sediments from Early Eocene subaerial to shallow-marine sediments. Towards the north and northeast, the basin is covered by a thick sequence of Middle–Late Miocene subaerial basalt and associated volcaniclastic sediments. The basin is transected by numerous fault zones, which were studied to help interpret the basin evolution (Fig. 3).

During this work we found that the stratigraphy of Gürer (l994) (see Fig. 5) remains largely applicable to the Hekimhan Basin, with the modifications as shown in Fig. 5. One important difference, however, results from the discovery during this work of volcanogenic rocks within the Middle Eocene succession in several areas in the south of the basin (see Figs. 3 and 5).

4. Mesozoic carbonate platform and ophiolite-related lithologies

The Mesozoic carbonate platform and the Late Cretaceous ophiolitic rocks that underlie the Hekimhan Basin provide clues to the regional tectonic setting, which immediately preceded the initiation of the basin. The stratigraphically oldest unit, which is only locally exposed (see Fig. 5), is the carbonate platform, locally named the Geniz Formation. This is dated as Late Jurassic to Mid–Late Cretaceous based on calcareous microfossils (Gürer, l994). This unit is mainly composed of white to buff-coloured, well-bedded (typically ~50 cm thick beds), hard, recrystallised limestone, sparsely interbedded with thin marls. The limestones are interpreted as part of the Tauride carbonate platform, which has recently been studied in detail in adjacent areas (Robertson et al., 2013b). After Triassic rifting, the carbonate platform developed during passive subsidence of the Tauride–Anatolide continent (Demirtaşlı et al., l984; Perinçek and Kozlu, l984; Özgül, l997; Taslı et al., 2006; Robertson et al., 2013b). During the latest Cretaceous, the leading, northerly edge of the carbonate platform underwent emplacement of ophiolitic rocks, while shelf deposition continued further south into Early Eocene time (e.g. Özgül, l997; Mackintosh and Robertson, 2013; Robertson et al., 2013b).

Within the study area, the emplaced ophiolitic rocks occur in the form of ophiolite-related mélange, termed the Hocalikova Formation (Fig. 5), which is formed by a combination of sedimentary and tectonic processes. Tectonic mélange is represented by large (hundreds of metres) detached blocks (olistoliths) and dismembered thrust sheets, which were sheared and faulted into place. These units are dominantly harzburgite, dunite and wherlite (all typically serpentinised), coupled with gabbro and rare plagiogranite. In addition, associated sedimentary mélange consists of debris-flow deposits that comprise relatively small blocks (tens of metres) and clasts (metres or less) of ultramafic and

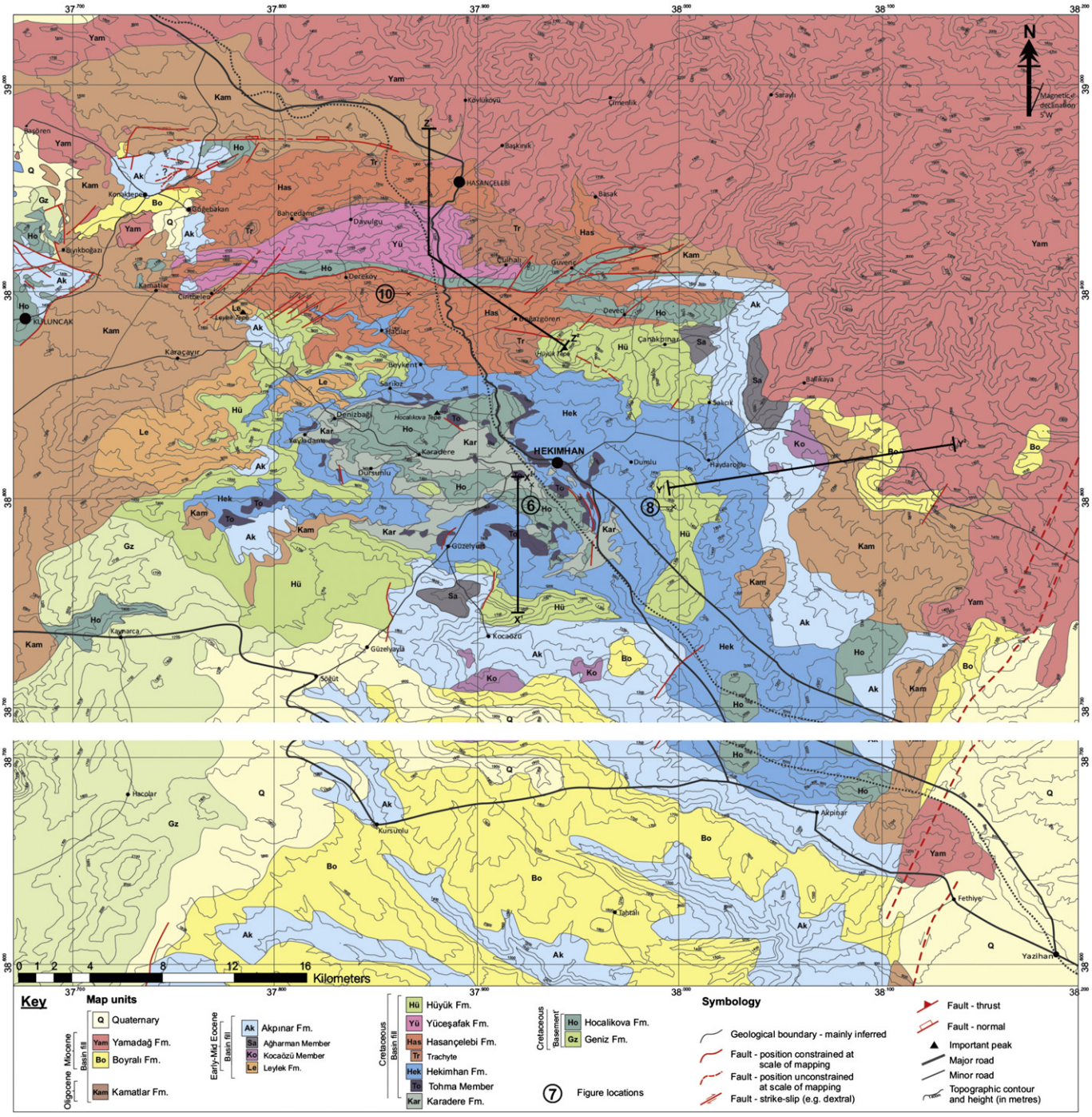

Fig. 3. Geological map of the Hekimhan Basin, compiled from sources specified in the text with additional data from this work. The geology is superimposed on the regional topography and the main roads. The locations of three partial sections across the basin are marked as black lines.

mafic ophiolitic lithologies, commonly dolerite and basalt, set in a sheared muddy–sandy matrix.

Similar dismembered ophiolitic rocks and massive debris flow-deposits were widely emplaced over the Tauride carbonate platform rocks throughout the Eastern Tauride region. Specifically, dismembered ophiolites and mélange were emplaced onto the Tauride platform in the Gürün area, to the west of the Hekimhan Basin during Campanian–Maastrichtian time (Perinçek and Kozlu, l984). The oceanic material is interpreted to have accreted above a northward-dipping subduction zone followed by its southward emplacement onto the northerly, distal edge of the Tauride carbonate platform during latest Cretaceous time (Robertson et al., 2013b).

5. Development of the Hekimhan Basin

The development of the Hekimhan Basin is discussed below as successive time slices.

5.1. Latest Cretaceous basin development

5.1.1. Latest Cretaceous non-marine deposition

The first post-ophiolite emplacement sediments are reddish-brown, non-marine sandstones and pebbly sandstones, termed the Karadere Formation (Fig. 5). The ophiolitic mélange (Hocalikova Formation) acted as a source for much of this sedimentary material. The sediments

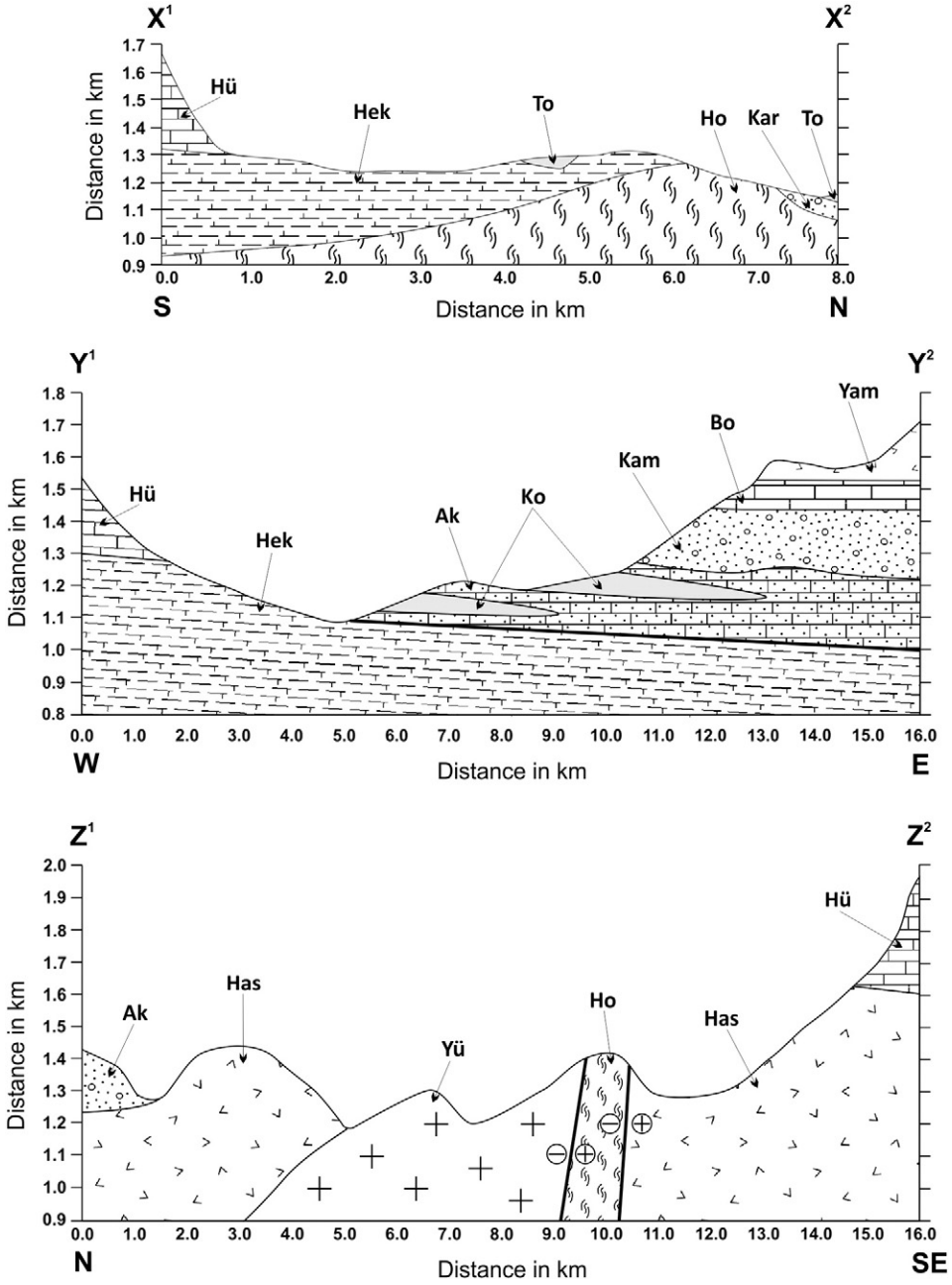

Fig. 4. Three partial sections across the Hekimhan Basin showing key stratigraphical and structural relationships (see Fig. 3 for locations). Ho, Hocalıkova; Kar, Karadere; To, Tohma; Hek, Hekimhan; Has, Hasançelebı; Hü, Hüyük; Yü, Yuceşafak; Ak, Akpınar, Ko, Kocaözü; Kam, Kamatlar; Bo, Boyralı; Yam, Yamadağ.

were deposited in a braided fluvial system, as indicated by the erosive, channelised and cross-bedded nature of many of the beds, coupled with clast-imbrication and ubiquitous clast rounding (see Fig. 6). Local changes in sediment thickness largely reflect differences in the relict palaeotopography, including 'highs' and 'lows', some of which were influenced by fluvial incision. Many packages of beds (e.g. ~8 km SW of Hekimhan) exhibit distinctive wedge-shaped geometries that are suggestive of deposition along an active extensional fault zone. Palaeocurrents measured from the south of the basin are directed ~northwards and ~westwards (Fig. 6, inset). The palaeocurrent data and the wedge-shaped facies geometry are inferred to reflect the onset of extension within the basin, when considered with other aspects of the basin evolution (see below).

5.1.2. Maastrichtian marine transgression

The Late Maastrichtian was characterised by marine transgression, as indicated by the appearance of rudist-rich patch reefs. These are designated as the Tohma Member of the Hekimhan Formation in our revised stratigraphy (Fig. 5). In different local areas (e.g. in the vicinity of Hekimhan) rudist reefs developed on elongate topographic highs (Fig. 7a) made up of carbonate platform and also on ophiolite-related 'basement' units (Geniz and Hocalikova Formations). The rudists grew on top of each other to form elongate mounds, up to 15 m high and several hundred metres long. Rudist bivalves flourished in many areas of Turkey during Late Cretaceous time (Özer, 2010) before becoming extinct at the Cretaceous–Tertiary boundary (Steuber and Loser, 2000).

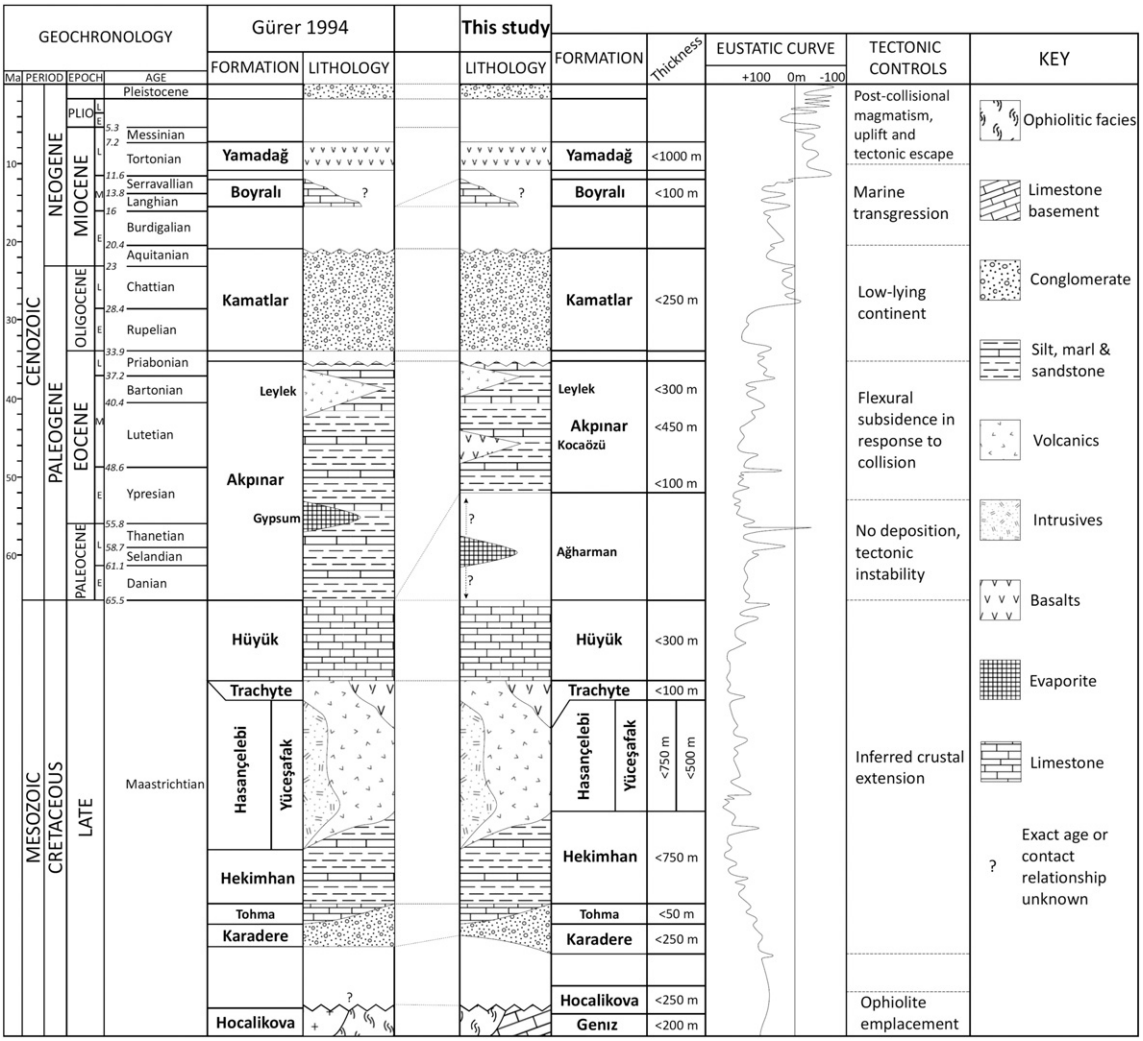

Fig. 5. Previous and revised stratigraphic nomenclatures of the Hekimhan Basin. The revised stratigraphy (this study) takes account of improved knowledge of the Mesozoic carbonate platform and emplaced ophiolite-related mélange (Robertson et al., 2013b), the dating of microfossils during this work and also of recent radiometric dating of Miocene volcanic rocks (Gürsoy et al., 2011). A global eustatic sea level curve (Miller et al., 2005) is included on the right to aid discussion of the controls of sediment deposition (i.e. tectonics versus sea level change). The main inferred controls of deposition are also indicated.

The initial shallow-marine deposition was followed by intense subsidence, still within the Maastrichtian, as indicated by a profound change from continental fluvial red beds (Karadere Formation) and shallow-marine rudist reefs to deeper-marine marl and calcarenite that form much of the Hekimhan Formation (see Figs. 5 and 8). Representative samples of the carbonate lithologies were studied for calcareous microfossils and the resulting taxonomic list is given in Table 1. Some age-diagnostic species are shown in Fig. 9.

The marls are rich in planktic foraminifera (e.g. Fig. 9a; e.g. *Globotruncanita* sp.) whilst the calcarenites contain abundant benthic foraminifera, together with fragmented bivalves, gastropods, echinoids and coral. Graded beds, laminated tops and occasional ripple lamination within calcarenites are indicative of deposition by turbidity currents and mass-flow processes (e.g. interval of 90–108 m in Fig. 8). The calcarenites were transported downslope as high concentration gravity flows from a shelf-depth setting. Vertical burrows within bioturbated calcarenites are locally infilled with glauconite, which is typical of transgressive shelf/slope settings (e.g. Odin, 1988). The 'background' sediment interbedded with the bioclastic gravity flows is mostly calcareous marl rich in planktic foraminifera.

Randomly orientated fungid corals are locally common within medium-grained to pebbly calcarenite. These solitary corals are predominantly intact but show no preferred orientation within coarse bioclastic carbonates. The fungid-bearing calcarenites are interpreted as mass-flow deposits that were triggered by gravity collapse or storm events. Fungid corals are inferred to have thrived under conditions similar to modern tropical corals (Matthai, 1948).

Continuing marine transgression resulted in the deposition of relatively deep-water hemipelagic marls throughout much of the basin. In places ~20 km SE of Hekimhan (to the north of Akpınar) the hemipelagic marls are interbedded with debris-flow deposits consisting almost entirely of reworked rudist fragments. Towards the centre and north of the basin (i.e. around Hasançelebi), the marls are organic-rich (black) and contain partially pyritised large bivalves. These sapropelic horizons are laterally extensive, up to 50 m thick and locally include up to 50 cm thick lenses of black, pebbly conglomerates with subrounded clasts composed of ophiolitic material. Localised downlaps and erosive surfaces are common within the organic-rich horizons. The sapropelic horizons are believed to represent isolated topographic depressions that formed within the deeper parts of the basin, where circulation was restricted, during a time of extension-related tilting and subsidence.

Syn-sedimentary deformation commonly affected the interbedded marls and calcarenites of the Hekimhan Formation. For example, competent beds of calcarenite have commonly slipped over less competent hemipelagic marls. Isolated, 'rafted blocks' of calcarenite occur within

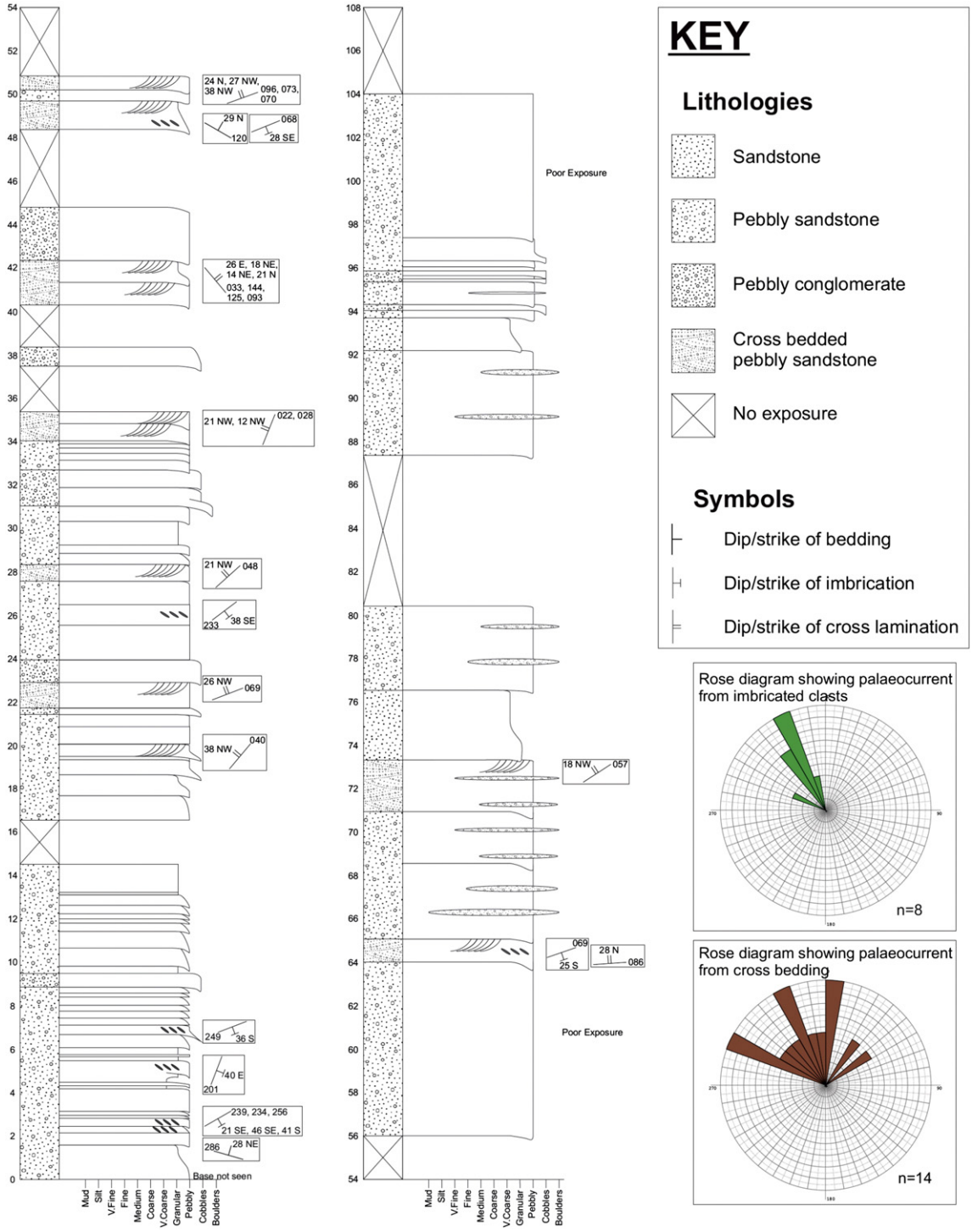

Fig. 6. Measured sedimentary log of part of the Maastrichtian Karadere Formation. See text for discussion and Fig. 4 for location.

deformed marl (Fig. 7c), some of these being crudely imbricated (Fig. 7d). The axes of slump folds measured in the south of the basin indicate a northward direction of sediment movement (Fig. 7e), suggesting that the basin deepened towards the north, at least locally. The existence of the various gravity-flow deposits supports an active tectonic control on basin formation during the Maastrichtian.

The uppermost levels of the Hekimhan Formation are characterised by the deposition of hemipelagic marls (~10 m-thick), followed by an abrupt appearance of shallow-marine limestones (Fig. 7b).

5.1.3. Volcanogenic rocks

In the northerly parts of the basin the Maastrichtian sedimentation was contemporaneous with the formation of a thick pile (~750 m) of volcanogenic rocks, known as the Hasançelebi Formation (Fig. 5). This is an association of extrusive–intrusive igneous rocks and associated clastic sediments (see Fig. 10). The extrusive volcanic rocks are mainly basaltic lava breccia, pillow lava and massive lava.

Lava breccia is the most abundant component of the Hasançelebi Formation (e.g. as exposed half way along the highway between

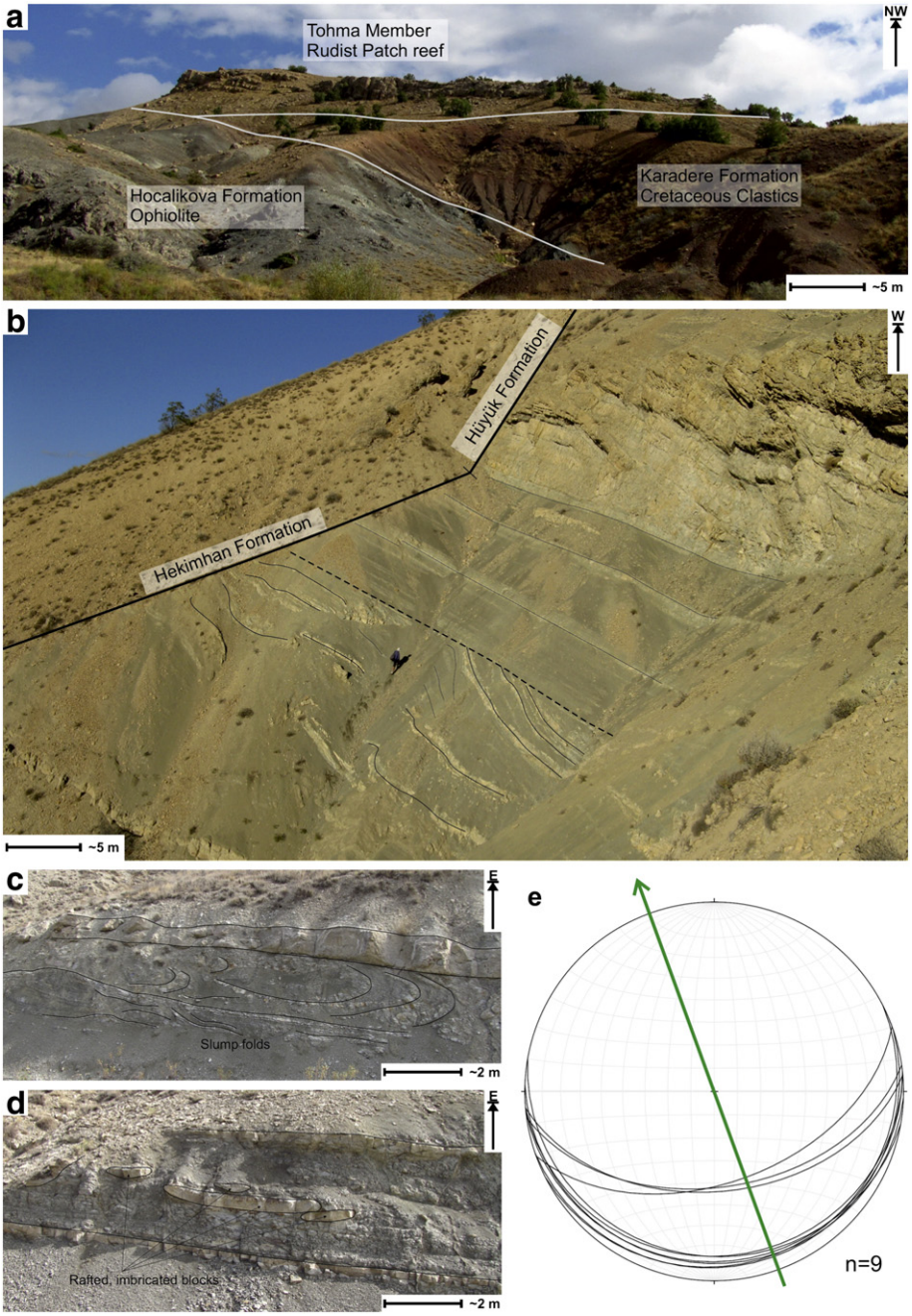

Fig. 7. Field photographs. (a) Red continental clastics of the Maastrichtian Karadere Formation onlapping the ophiolitic mélange; both of these are unconformably overlain by a rudist-bearing patch reef (Tohma Member). (b) Maastrichtian Hekimhan Formation showing syn-sedimentary deformation (below the dashed line), overlain by undeformed beds. The massive unit in the upper right is limestone of the Hüyük Formation (figure for scale in centre). (c) Slump folds within marl layers overlain by a relatively undeformed calcarenite bed. (d) Rafted and imbricated blocks of competent (lithified) calcarenite within marl. (e) Stereonet showing great circles of slump fold axial planes. Arrow indicates down-slope movement direction of the slumped material ($n = 9$).

Hekimhan and Hasançelebi). Clasts are angular, ranging from pebble- to cobble-sized. Pillow basalts and massive lava flows commonly grade laterally into lava breccia along the same stratigraphic horizon, consistent with an origin as flow-front breccia. Individual basaltic lava flows range in thickness from ~10 to ~60 cm, as observed at variable intervals within the Hasançelebi Formation, for example ~1 km east of Hacılar (midway between Hekimhan and Hasançelebi). Individual pillows range in size from <0.5 to ~1 m in diameter. Elongate bolster pillows and lava tubes rarely occur associated with pillow lavas.

Based on thin section observations, the basalts are clinopyroxene and plagioclase-phyric, coupled with clinopyroxene and plagioclase microphenocrysts, all set in a finely crystalline mesostasis. Plagioclase phenocrysts and microphenocrysts within some of the lava flows show flow alignment.

The pillowed and massive basalt flows locally contain inter-lava marl from which planktic foraminifera yielded a Maastrichtian age (Table 1; sample MB08-3). The Maastrichtian volcanic rocks erupted subaqueously, probably at depths of up to several hundred metres, as suggested by the abundance of planktic foraminifera (compared to benthic foraminifera) within the interbedded marls. Subsidence was most intense in the north of the basin, where water depths were greatest based on facies and micropalaeontological evidence. Light grey, fine-grained tuff was observed north of Hasançelebi, interbedded with graded volcaniclastic sandstones. The tuffs are interpreted as air-

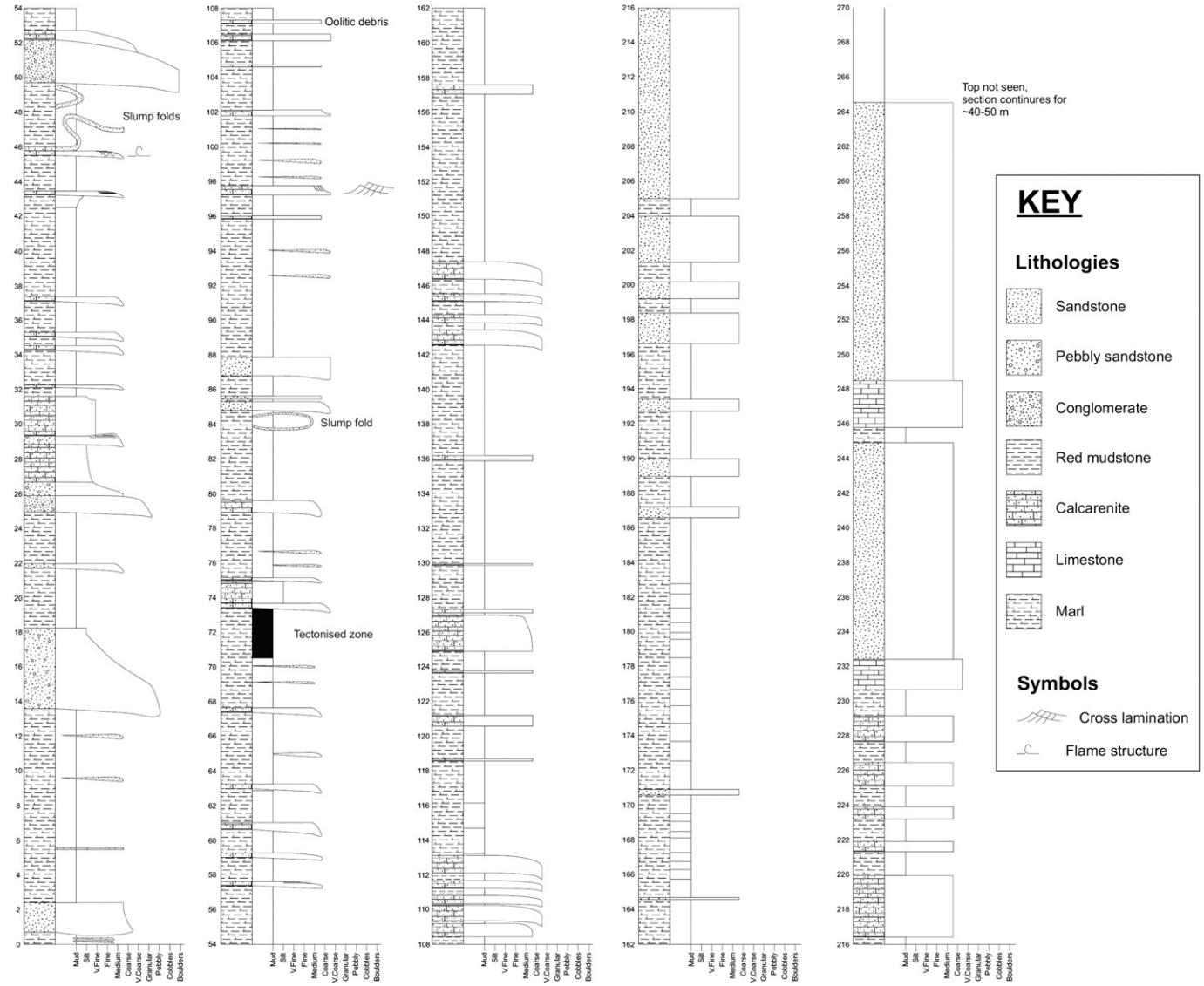

Fig. 8. Measured sedimentary log of part of the Maastrichtian Hekimhan Formation. See text for discussion and Fig. 4 for location.

fall deposits, indicating that some volcanism took place subaerially or possibly in a very shallow sea.

To shed light on their eruptive setting, 18 samples of volcanic rock were analysed by X-ray fluorescence (XRF) using the methods described by Fitton et al. (1998). Representative analyses are shown in Table 2, while the complete data set is included in an on-line supplementary publication. In the total alkalis versus silica (TAS) rock classification diagram (La Maitre et al., 2002; Fig. 11) most of the lavas plot within, or near, the basaltic-trachyandesite, trachy-andesite, andesite, basaltic andesite and basalt fields. A multi-element 'spider' plot normalised against N-MORB (Fig. 12) shows that the volcanic rocks resemble within-plate basalts (WPB) (Pearce, 1982). These rocks exhibit a strong enrichment of the large ion lithophile elements (LILEs), i.e. Sr to Ba and light rare earth elements (LREEs), i.e. La to Ce. This trend could either be of primary magmatic origin or reflect alteration. The high field strength elements (HFSEs) Nb, Zr and Ti are slightly enriched compared to MORB, whereas those on the right hand side of the plot (Sc, Ni, Cr) are relatively depleted. The within-plate basalts, therefore, show marked

Table 1
Calcareous microfossils identified in the Maastrichtian Hekimhan Formation.

Hekimhan Formation (Maastichtian)				
Samples	Rock type	Benthic Foraminifera	Planktic Foraminifera	Age
MB08-3	Mudstone	–	*Rugoglobigerina rugosa, Globotruncanita conica, Globotruncana arca, Pithonella ovalis*	Late Maastrichtian
MB08-27	Micrite	–	*Globotruncanita stuartiformis, Contusotruncana* sp., *Rugoglobobigerina* sp., *Heterohelix* sp., *Archaeoglobigerina* sp.	Maastrichtian
MB08-41	Micrite	–	*Rugoglobigerina rugosa, Globotruncana ventricosa, Pseudotexularia* sp.	Maastrichtian
MB08-156	Sandy limestone	*Sirtina orbitoidiformis, Pseudovalvulineria clementiana, Orbitoides* sp., *Lepidorbitoides* sp.	*Globotruncanita* sp., *Pithonella ovalis, Calcisphaerula inniminata*	Late Maastrichtian
MB09-H47	Marly limestone	*Pseudovalvulineria clementiana*	*Rugoglobigerina macrocephala, Globotruncanita* sp., *Pseudotextularia* sp., *Pithonella ovalis,*	Late Maastrichtian

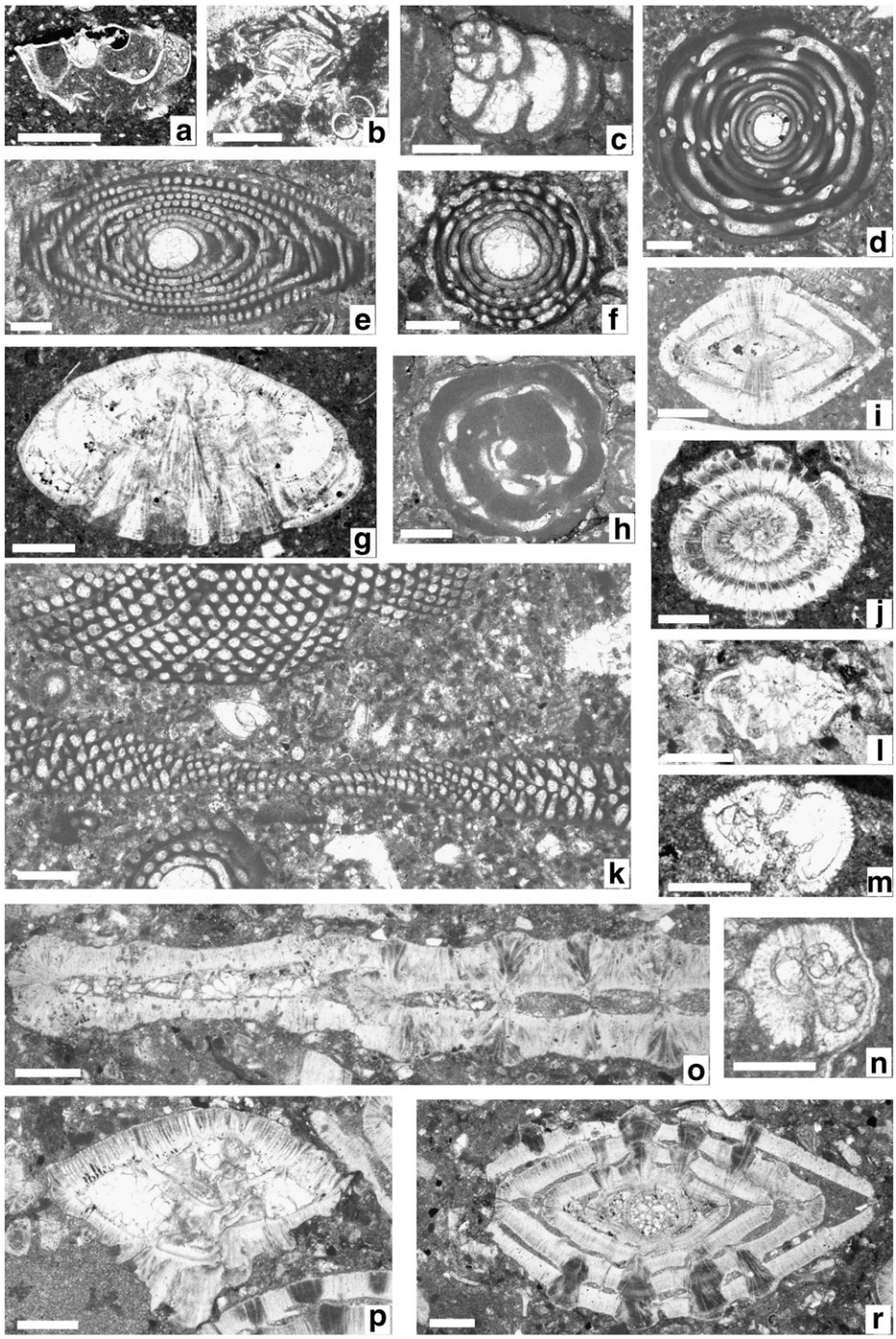

Fig. 9. Some age-diagnostic planktic and benthic foraminifera identified from the Maastrichtian and Eocene marine facies of the Hekimhan Basin. (a) *Globotruncanita* sp., sample MB08-27 (Maastrichtian, Hekimhan Formation). (b) *Sirtina orbitoidiformis*, sample MB09-H91 (Maastrichtian, Hüyük Formation). (c) *Pfendericonus* sp., MB10-66. (d) *Alveolina (Glomalveolina) levis*, sample MB10-83. (e and f) *Alveolina (Glomalveolina) subtilis*, sample MB10-122. (g) *Lockhartia haimei*, sample MB10-80. (h) *Alveolina (Alveolina)* cf. *aragonensis*, sample MB10-66. (i and j) *Nummulites* cf. *minervensis*, sample MB10-80. (k) *Orbitolites complanatus*, MB10-83 (c-k Ilerdian, Early Eocene, Akpınar Formation). (l) *Neorotalia vienotti*, sample MB10-38. (m) *Acarinina bullbrooki*, sample MB10-69. (n) *Globigerinatheka* sp., sample MB10-69. (o) *Ranikothalia* sp., sample MB10-69. (p) *Medocia blayensis*, sample MB10-69. (r) *Nummulites* cf. *striatus*, sample MB10-113 (l–r Lutetian, Mid Eocene, Akpınar Formation). Scale bars: 0.2 mm.

enrichment in immobile incompatible elements relative to MORB and a range of compatible elements (e.g. Cr and Ni). These trends are compatible with modest fractional crystallisation of the parental basaltic magma.

Niobium exhibits a small negative anomaly compared to the normalised values of Th and La, which can be attributed to mantle-source enrichment during subduction (Dilek and Furnes, 2009; Keskin et al., 1998; Pearce et al., 1990). Niobium is relatively immobile in aqueous fluids and is thus relatively depleted in magmas generated above subduction zones (Baier et al., 2008; Pearce, 1982). Metasomatic processes and also the assimilation of crustal rocks can in some circumstances influence Nb content (Keskin et al., 1998, 2008; Pearce and Cann, 1973). However, it is likely that the negative Nb anomaly in the basalts reflects a subduction-influenced source. Similar negative Nb anomalies have

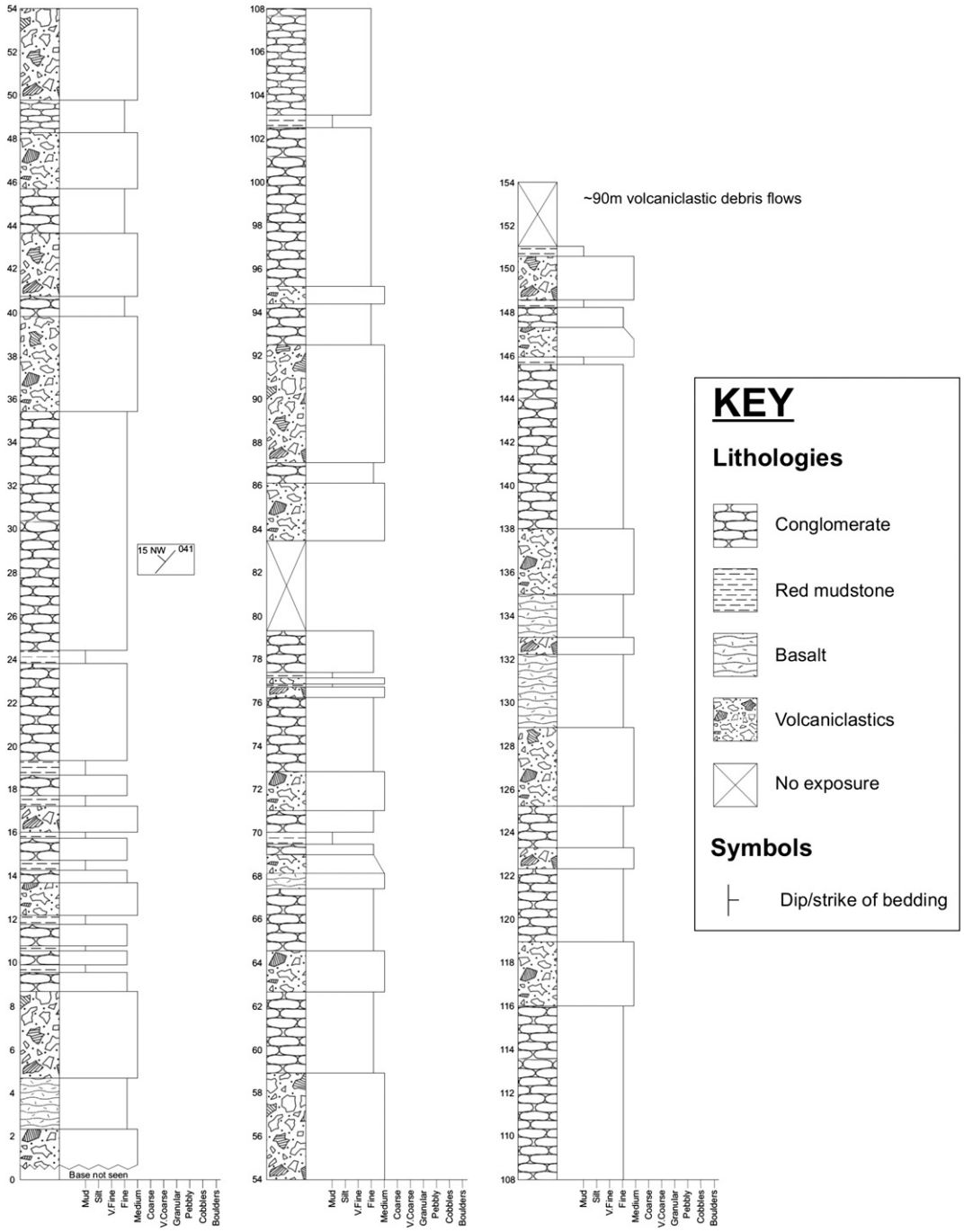

Fig. 10. Measured log of part of the Maastrichtian Hasançelebi Formation. See text for discussion and Fig. 4 for location.

been attributed to a subduction-influenced source in neighbouring basins, including the Ülükışla Basin (Clark and Robertson, 2002, 2005) and the Çankırı Basin (Nairn et al., 2013).

A likely cause of the subduction signature in the Maastrichtian basaltic rocks was regional northward subduction from the Southern Neotethys, beneath the Tauride–Anatolide continental unit (above which sits the Hekimhan Basin). An additional possibility that cannot be discounted is that the subduction signature was inherited from mantle lithosphere that was affected by an earlier (i.e. pre-Late Cretaceous) subduction event in the region. It must also be noted that, in principle, subduction fluids could have resulted from southward subduction beneath the Tauride–Anatolide continent, although this option is not favoured in most recent tectonic interpretations.

5.1.4. Mudrocks and fine-grained sandstones

More light is shed on the tectonic setting of the volcanogenic rocks by study of the associated sandstones and mudrocks. Do these indicate regionally widespread magmatism during the Maastrichtian, for example?

The volcanogenic rocks (flows and breccias) are locally interbedded with dark-grey to dark-red, coarse grained, texturally immature volcaniclastic sandstones (1–5 cm thick beds). The sandstones are mostly composed of ferromagnesian minerals and hyaloclastite. Sedimentary grading and parallel-laminated tops of beds suggest a turbiditic origin. The volcaniclastic sandstones are interpreted as subaqueously erupted material that was reworked into local depocentres as gravity flows. In addition, there are occurrences of reddish, finely laminated,

Table 2
Representative chemical analyses of basalt and volcaniclastic sediments from the Maastrichtian Hasançelebi Formation, syenite from the Maastrichtian Yüceşafak Member, basalt samples from the Eocene Kocaözü Member and andesite from the latest Eocene–Oligocene Leylek Member. LOI, loss on ignition; major elements as percentages; minor elements in parts per million (ppm). Data for all of the samples analysed are available in the on-line supplementary publication.

Hekimhan Formation sample				Yüceşafak Member				Kocaözü Member						Leylek Member			
Sample	MB08-8	MB08-20	MB08-228	MB08-17	MB10-97	MB10-111a	MB10-111b	MB10-70a	MB10-70b	MB10-70c	MB10-84a	MB10-84b	MB10-84c	MB10-34a	MB10-34b	MB10-51	MB10-120
Latitude	38.8793	38.9416	38.9314	38.9416	39.0017	38.9143	38.9143	38.8190	38.8190	38.8190	38.7316	38.7316	38.7316	38.8778	38.8778	38.8914	38.8632
Longitude	37.8955	37.8750	37.8792	37.8750	37.7606	37.8779	37.8779	38.0402	38.0402	38.0402	37.8932	37.8932	37.8932	37.7877	37.7877	37.8152	37.8057
Majors (%)																	
SiO_2	55.08	49.99	58.05	65.66	68.74	59.07	58.30	62.97	68.65	51.48	52.65	44.39	51.12	70.57	69.48	54.90	59.98
Al_2O_3	18.47	16.91	17.70	17.18	16.31	16.77	16.38	19.25	16.27	18.45	17.99	13.94	15.42	16.45	16.48	18.58	17.88
Fe_2O_3	4.59	7.50	3.14	0.41	2.91	2.04	2.29	4.96	1.54	6.99	9.54	6.14	10.04	1.90	1.92	6.55	5.91
MgO	2.95	6.08	2.93	0.15	1.23	4.29	4.99	1.87	1.22	8.00	5.13	16.59	3.15	1.05	1.34	1.43	3.61
CaO	9.27	10.04	6.00	6.13	3.83	7.66	8.53	6.77	4.53	9.20	4.64	17.34	11.01	1.84	2.28	8.16	6.08
Na_2O	5.92	4.79	7.86	9.72	4.15	7.45	7.52	3.77	3.01	3.89	6.79	0.00	2.50	5.78	6.10	3.73	3.49
K_2O	1.07	2.93	1.96	0.22	2.24	1.79	1.01	1.81	1.58	0.70	0.50	0.00	0.70	1.94	1.87	4.38	2.20
TiO_2	1.96	1.38	1.75	0.39	0.38	0.90	0.93	0.75	0.30	0.84	1.58	0.16	0.58	0.34	0.34	1.67	0.62
MnO	0.15	0.09	0.04	0.04	0.04	0.05	0.05	0.04	0.02	0.10	0.16	0.12	0.13	0.02	0.03	0.13	0.10
P_2O_5	0.52	0.30	0.58	0.10	0.16	0.00	0.00	0.18	0.10	0.11	0.60	0.00	0.05	0.13	0.15	0.46	0.14
LOI	6.34	5.12	4.42	4.70	0.73	3.47	3.59	1.49	1.57	1.28	2.76	2.82	2.67	1.21	1.10	4.72	1.39
Total	99.51	99.22	99.57	99.98	99.90	100.04	99.66	99.33	100.49	99.43	99.54	99.29	99.61	99.35	99.93	99.69	99.44
Total – LOI	93.18	94.09	95.16	95.28	99.17	96.57	96.07	97.84	98.92	98.15	96.78	96.47	96.94	98.14	98.83	94.97	98.05
Trace (ppm)																	
Zn	228.80	47.00	80.60	n.d.	36.20	2.10	0.90	60.00	55.40	102.30	84.00	83.60	84.60	31.20	31.30	117.30	47.70
Cu	1366.00	29.40	41.90	6.00	13.60	3.40	3.60	32.80	46.20	9.30	71.40	73.80	66.40	18.20	17.20	62.90	13.70
Ni	25.00	48.00	86.00	n.d.	8.00	13.70	17.10	126.60	131.30	32.00	56.50	55.10	57.40	22.00	24.30	25.80	9.10
Cr	−22.40	57.60	137.40	n.d.	13.70	0.00	3.90	275.00	288.20	128.50	182.20	178.70	181.10	16.20	15.50	20.60	33.10
V	206.10	197.30	179.80	15.50	42.30	22.50	22.90	200.00	188.90	151.30	223.70	228.50	224.20	36.90	38.90	581.80	139.80
Ba	277.50	3018.70	294.40	366.90	382.40	717.10	439.80	221.10	211.50	1144.70	389.60	388.60	381.60	551.90	530.80	22.70	421.70
Sc	18.90	23.10	23.10	n.d.	5.10	3.10	6.80	28.50	26.80	18.80	30.70	29.70	30.00	5.70	4.30	48.00	20.50
La	38.70	52.10	17.40	31.30	28.40	49.70	51.40	12.90	10.00	85.40	22.20	21.90	22.60	20.20	18.00	1.40	19.30
Ce	75.00	61.20	35.10	77.70	48.80	104.20	109.70	28.00	26.50	144.40	42.70	44.30	43.10	28.00	29.70	11.70	39.30
Nd	33.30	12.90	20.40	34.70	17.70	44.30	48.20	13.40	14.50	55.30	20.60	18.90	20.10	12.40	10.50	10.10	16.20
U2	1.60	7.50	1.10	8.00	2.30	8.80	7.10	0.30	0.10	4.60	2.50	2.10	2.30	1.50	1.60	0.10	1.60
Th	7.20	4.00	4.50	26.00	7.60	17.70	16.60	2.30	2.90	20.50	7.70	7.90	7.70	5.50	5.50	n.d.	7.20
Pb	28.20	13.00	5.70	0.30	10.00	1.20	1.80	3.20	4.50	15.50	8.30	9.00	9.10	5.70	7.10	2.00	4.40
Nb	46.60	15.30	14.60	34.10	10.80	56.50	54.40	8.80	8.80	24.40	12.60	12.80	12.60	12.20	12.20	1.40	10.10
Zr	213.80	134.40	172.90	372.40	193.30	375.00	387.20	94.10	94.20	157.30	153.90	156.10	153.60	95.90	95.80	82.50	119.10
Y	37.30	23.90	28.40	34.00	12.60	50.40	58.40	22.00	21.80	24.60	28.20	28.50	28.20	9.90	6.60	32.20	20.10
Sr	410.60	3383.10	429.80	137.70	322.00	309.50	319.90	315.10	311.70	862.30	308.90	308.90	304.90	446.40	515.30	172.40	277.20
Rb	58.20	113.40	23.10	n.d.	46.50	22.80	12.30	9.60	8.20	57.40	46.10	47.70	46.20	43.30	42.00	4.00	63.70

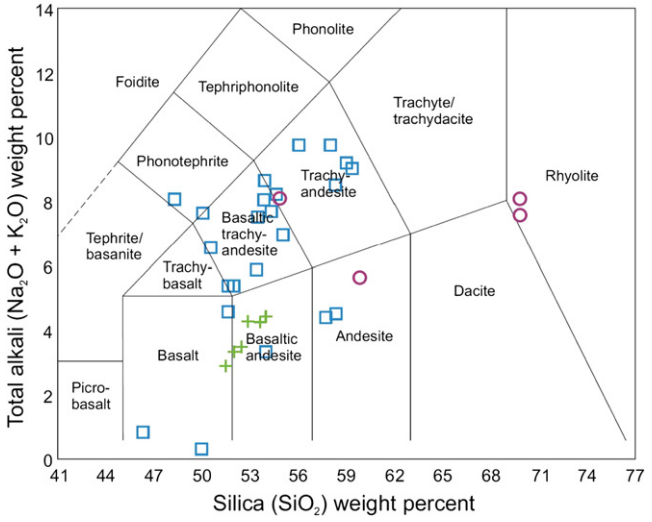

Fig. 11. Volcanic rock classification diagrams utilising total alkalis (Na2O + K2O) versus silica (SiO2) (Le Maitre et al., 1989, 2002). Squares, Maastrichtian Hasançelebi Formation; crosses, Eocene Kocaözü Member; circles, Eocene Leylek Member. Q = normative quartz; Ol = normative olivine. See text for explanation.

unfossiliferous mudstone, which generally occur as thin intercalations (1–20 cm) between pillow lavas, lava flows or coarse-grained volcaniclastic sandstones. The mudstone includes numerous manganese concretions (<3 cm in diameter). These mudrocks are often associated with peperites that formed when lavas erupted onto the fine-grained sediment (e.g. ~1 km east of Hacılar).

Six samples of the red inter-lava mudstone were also chemically analysed, using the same methods as for the volcanic rocks discussed above (see Table 3). The data are plotted as a spider diagram, normalised against the average composition of the Hasançelebi Formation basalt in Fig. 13a. Ti and Nb, two elements that are relatively unaffected by alteration, are much lower than in the basalts. In addition, the same data were normalised against the average composition of continental crust (McLennan et al., 2006) (Fig. 13b). This shows a similarity for some elements (e.g. Sc, Ti, Cr (in 2 samples), Zr, Nb and Th), whereas Rb and Ba are strongly depleted, while V, Cr (in 2 samples), Ni and Pb are markedly enriched. Continental crust and not just volcanogenic material, therefore, appears to have contributed to the composition of the fine-grained sediments with the volcanogenic sequence.

Table 3
Geochemical analyses of six samples of volcaniclastic sediments from the Maastrichtian Hasançelebi Formation, determined by x-ray fluorescence using the method specified in Fitton et al. (1998). LOI, loss on ignition; major elements as percentages, minor elements in parts per million (ppm).

Sample	MB08-09	MB08-10	MB08-11	MB08-12	MB08-14	MB08-49
Latitude	38.8793	38.8793	38.8793	38.8793	38.8793	38.8802
Longitude	37.8955	37.8955	37.8955	37.8955	37.8955	37.8945
Majors (%)						
SiO_2	43.51	43.89	53.69	53.56	55.53	54.59
Al_2O_3	9.54	13.47	16.52	11.68	14.86	16.31
Fe_2O_3	30.73	21.24	13.42	20.13	9.96	10.65
MgO	5.00	7.73	5.56	3.74	7.39	5.55
CaO	3.75	4.77	2.12	2.55	6.33	4.81
Na_2O	0.65	0.92	0.94	0.65	4.49	6.79
K_2O	1.70	2.66	4.67	2.75	0.25	0.24
TiO_2	0.42	0.61	0.80	0.50	0.86	0.76
MnO	4.27	4.36	1.92	3.93	0.27	0.20
P_2O_5	0.42	0.36	0.38	0.50	0.06	0.07
LOI	4.52	6.38	6.04	5.50	5.05	4.94
Total	99.30	99.83	99.51	99.51	99.69	99.37
Total – LOI	94.78	93.45	93.47	94.01	94.64	94.43
Trace (ppm)						
Zn	298.00	270.70	158.80	216.40	86.90	64.90
Cu	156.50	3783.60	1427.80	619.90	675.90	62.30
Ni	249.90	310.50	201.80	246.80	98.80	121.10
Cr	83.70	109.40	158.70	55.50	354.20	409.40
V	780.80	356.20	143.00	302.30	269.80	201.80
Ba	108.50	227.40	149.10	173.30	30.00	36.30
Sc	18.30	24.50	32.90	21.00	45.00	42.30
La	86.20	75.90	56.30	76.80	n.d.	4.70
Ce	72.00	86.70	101.80	82.20	8.60	13.40
Nd	84.20	65.00	52.50	65.30	5.00	7.70
U2	0.70	0.10	0.80	0.10	n.d.	0.00
Th	2.60	5.40	9.10	3.90	n.d.	n.d.
Pb	150.60	61.50	51.40	138.60	4.90	11.00
Nb	9.70	10.80	14.50	10.50	1.30	2.30
Zr	115.60	109.90	127.70	105.10	43.90	43.30
Y	79.00	58.90	56.50	60.50	19.90	20.20
Sr	73.80	149.30	87.10	313.50	78.40	62.30
Rb	53.60	77.50	125.10	84.90	2.60	4.30

There was a ready source of terrigenous material in the surrounding Tauride continental crust. Chromium, together with V and Ni, is enriched in the volcaniclastic sediments relative to both average continental crust and average basalt of the Hasançelebi Formation. The likely

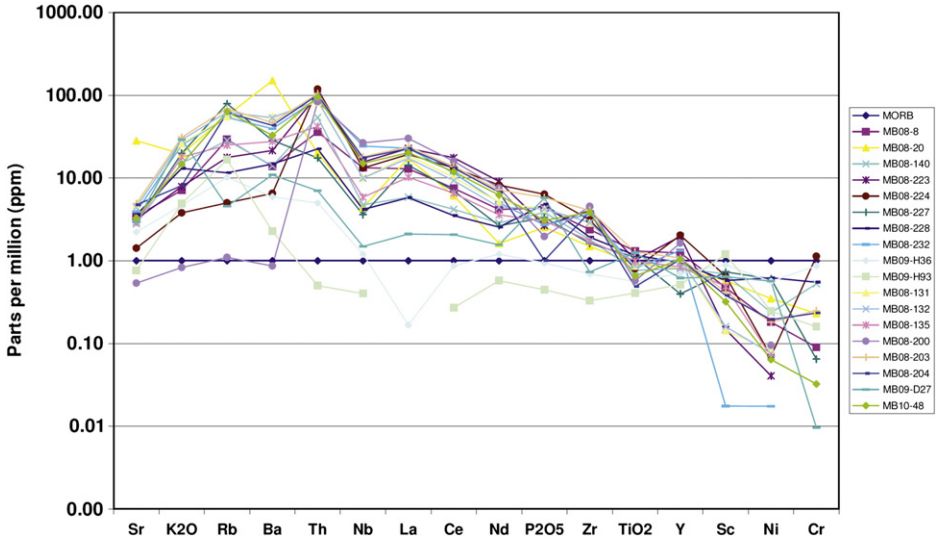

Fig. 12. Mid-ocean ridge basalt (MORB)-normalised spider diagrams for the Maastrichtian-aged Hasançelebi Formation basaltic rocks. Normalising values from Pearce (1982) and Saunders and Tarney (1984). See text for discussion.

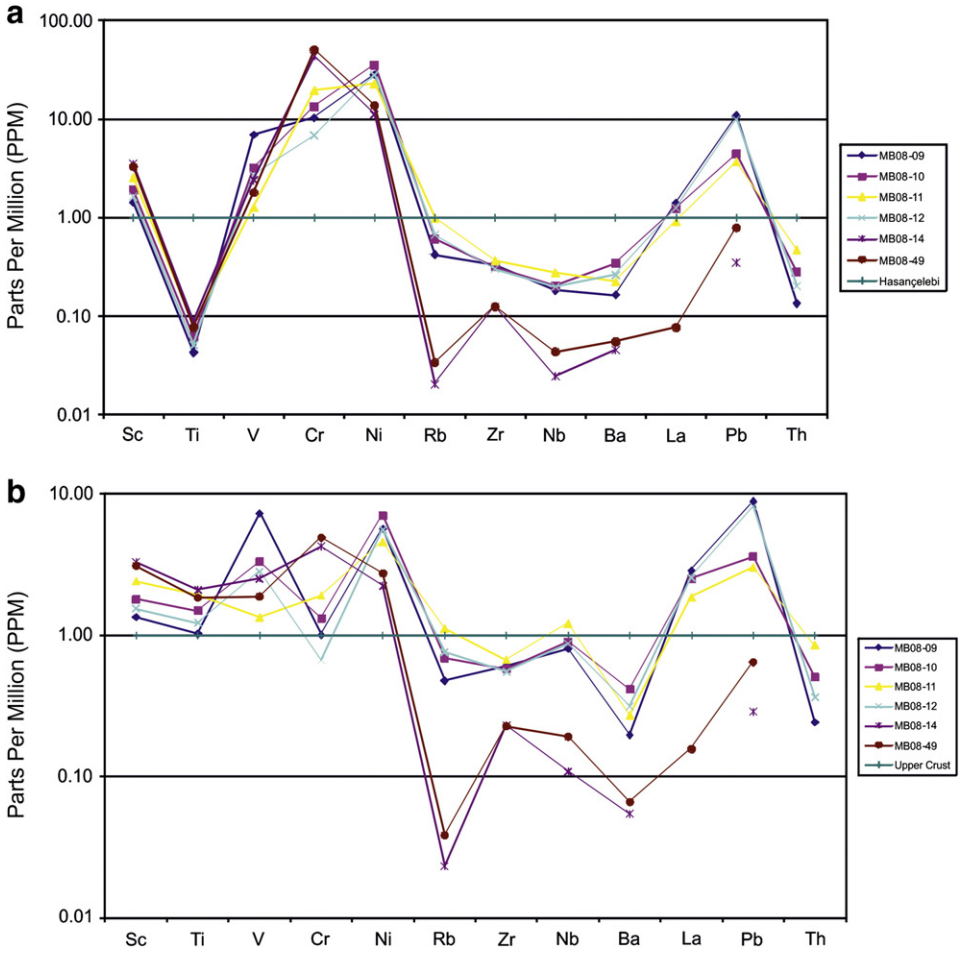

Fig. 13. (a) Spider plots of volcaniclastic sediments of the Maastrichtian Hasançelebi Formation, normalised against the average composition of basalt of the Hasançelebi Formation. (b) Same data normalised against average continental crust (normalising data in both plots from McLennan et al., 2006). See text for explanation.

source for the excess Cr and Ni, in particular, was the Late Cretaceous ultramafic ophiolitic rocks exposed beneath and around the Hekimhan Basin (Fig. 3). Similar enrichments of Cr and Ni elsewhere reflect erosion of ultramafic rocks, for example, bordering the Woodlark Basin in the SW Pacific (Robertson and Sharp, 2002).

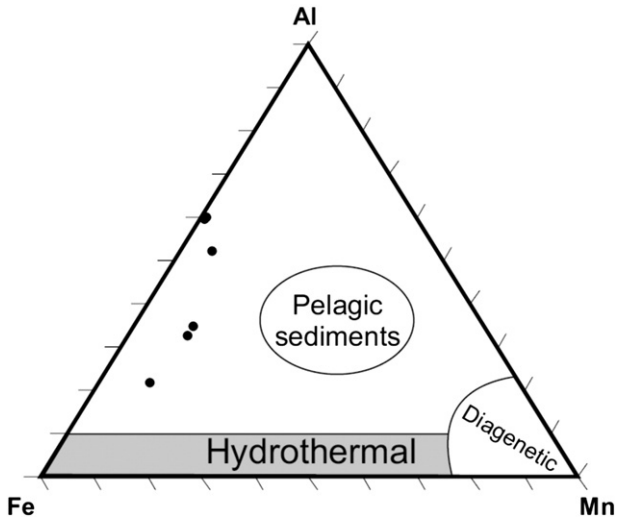

Fig. 14. Ternary plot showing the relative abundances of Al, Fe and Mn within red mudstones associated with the Maastrichtian volcanogenic rocks. The plot shows a relative abundance of Fe relative to Al, but depletion in Mn. The compositions of typical pelagic sediments, hydrothermal oxide sediments and diagenetic MN-rich sediments are indicated after Turekian and Wedepohl (1961).

The red mudstones are also distinctly metalliferous. On a ternary plot of Al plotted against Fe and Mn, Al ranges from ~40 to 70%, Fe from ~20 to 60% and Mn from ~0 to 10% (Fig. 14). The red mudstones, therefore, show a marked enrichment in Fe relative to Al and Mn in typical terrigenous or mafic-volcanic-derived muds. Bivariate plots (Fig. 15a) suggest that the Al, Ti, Cr and several other elements are mainly lithogenous in origin. Iron oxide (Fe_2O_3) and Al_2O_3 are inversely proportional (Fig. 15b), as are TiO_2 and Fe_2O_3 (Fig. 15c), suggesting that iron is independent of lithogenous input, whether terrigenous or volcaniclastic. The most obvious source for such iron enrichment is the dispersal and oxidation of sulphide particles to form fine-grained oxide sediments (e.g. Cann and Gillis, 2004). Additional evidence of hydrothermal alteration is present within the volcanogenic assemblage in the form of mineralised fracture networks (e.g. containing malachite and azurite). Vertical, hydrothermally altered zones are also present within marls and limestones, as marked by reddish, brownish, or black metalliferous oxide mineralisation, especially along fracture planes. Hydrothermal oxide deposits are commonly enriched in Mn as well as Fe (e.g. Cyprus umbers; Robertson and Boyle, 1983). However, Fe_2O_3 and MnO in the ferruginous mudstones are negatively correlated (Fig. 15d). This can be explained by the post-depositional mobilisation and loss of manganese within the muds, while the manganese was concentrated in the associated small spherical concretions.

The geochemical evidence suggests that the interlava volcaniclastic sediments formed from a mix of continental, ophiolitic and hydrothermal components, with little input directly from the associated basaltic rocks.

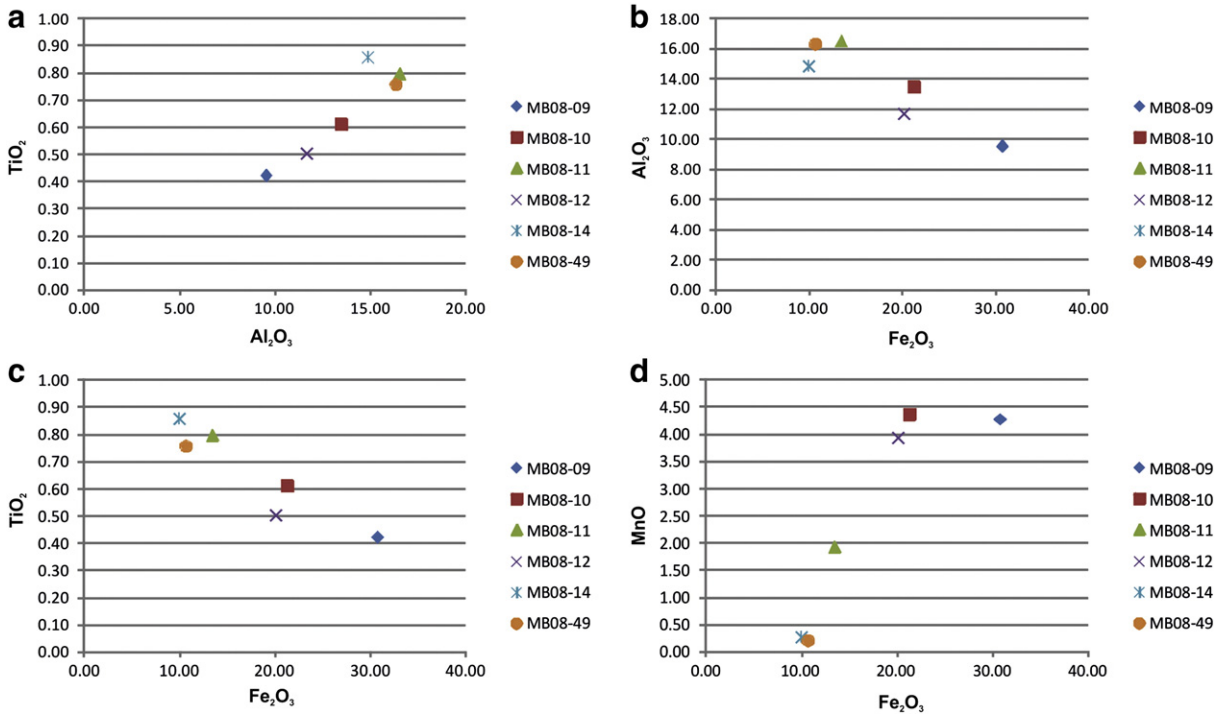

Fig. 15. Bivariate plots showing (a) Al2O3 vs. TiO2, (b) Fe2O3 vs. Al2O3, (c) TiO2 vs. Fe2O3, and (d) Fe2O3 vs. MnO. See text for explanation.

This is important because it indicates that the Maastrichtian volcanism was essentially localised within the basin, while continental crust and ophiolitic material was exposed to erosion round about. There is thus no evidence for contemporaneous arc magmatism in the surrounding geology, much of which is concealed by Neogene–Recent sediments and volcanics (MTA, 2002).

5.1.5. Alkaline intrusion

White, coarse-grained, holocrystalline, alkali feldspar-bearing syenite outcrops in the northern part of the Hekimhan Basin, known as the Yüceşafak Member (Fig. 5). This rock is up to 90% orthoclase feldspar with minor hornblende, quartz and biotite. Small amounts of olivine are also present. In many outcrops ferromagnesian minerals have been altered by metasomatic, hydrothermal, or weathering processes. Sulphide mineralisation is common, including malachite, azurite and chalcanthite. In some areas the syenite is dark-green to dark-grey which can be explained by the addition of nepheline. Some of the syenite shows radial crystallisation textures. Veins of pegmatitic syenite are present in places. In addition, there are isolated enclaves of more mafic intrusuive rocks. Isolated syenitic dykes that cut the basaltic rocks of the Maastrichtian Hasançelebi Formation are interpreted as relating to intrusion of larger plutonic bodies (Yüceşafak Member). Unfortunately, the two rock suites are not exposed in the same area. The main pluton has been interpreted as an oversaturated alkaline subtype of the cafemic association, suggesting a mantle-derived source (Ozgenç and Ilbeyli, 2009; Yılmaz et al., 1993),

To help determine the tectonic setting of magma intrusion, four samples of syenite were analysed by XRF using the methods indicated above. Geochemical analyses are given in Table 2. A rock classification diagram (Fig. 16) indicates that three samples are syenite-syeno-diorite, while one is granite-grano-diorite. The felsic I-type composition is indicative of a within-plate setting.

A single $^{40}Ar/^{39}Ar$ age determination of an orthoclase crystal from alkaline syenite (described as from Basoren village) has yielded a late Maastrichtian age of 65.2 ± 1.6 Ma (Leo et al., 1973), which is consistent with the age of basaltic volcanism in the Hekimhan Basin, as determined using microfossils (see above). However, an extrusive equivalent of the alkaline syenite has not been recorded within the basin. In addition, Kuşcu et al. (2011) have used $^{40}Ar/^{39}Ar$ and U-Pb geochronology to identify four separate phases of alteration of the alkaline syenite, ranging from ~74 to 68 Ma. These ages imply intrusion of the plutonic body (Yüceşafak Member) prior to latest Campanian time, thus predating the basaltic rocks within the Hekimhan Basin. The alkaline syenite intrusion could represent a precursor to the voluminous Maastrichtian-aged alkaline basaltic volcanism.

5.1.6. Maastrichtian basin infill

The Late Cretaceous sedimentary and igneous rocks, discussed above, are covered by fine to coarse-grained bioclastic carbonates and marls of the Hüyük Formation (Fig. 5), which varies in thickness across

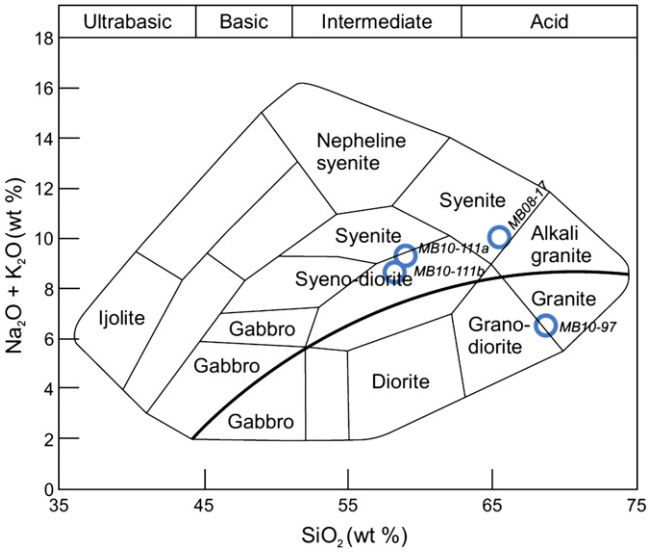

Fig. 16. Rock classification diagram for the intrusive plutonic rocks (Yüceşafak Member) (after Cox et al., 1979, as adapted by Wilson, 1989). The curved solid line subdivides alkalic from subalkalic rocks.

Table 4
Calcareous microfossils identified in limestones of the Hüyük Formation.

Hüyük Formation (Maastichtian)				
Samples	Rock type	Benthic Foraminifera	Planktic Foraminifera	Age
MB08-45	Sparry limestone	*Sivasella monolateralis, Orbitoides* sp., *Anomalina* sp.	–	Late Maastrichtian
MB08-151	Limestone	*Mississippina binkhorsti Orbitoides* sp., *Anomalina* sp.	–	Maastrichtian
MB08-160	Limestone	*Sirtina orbitoidiformis, Pseudovalvulineria clementiana, Chrysalidina* sp., *Lepidorbitoides* sp.	*Rugoglobigerina rugosa, Globotruncana falsostuarti, Globotruncanita* sp.	Late Maastrichtian
MB08-235	Limestone	*Sirtina orbitoidiformis,*	–	Late Maastrichtian
MB09-H91	Limestone	*Sirtina orbitoidiformis, Siderolites* sp., *Eponides* sp.	*Rugoglobigerina* sp., *Globotruncana* sp., *Pithonella ovalis*	Late Maastrichtian
MB10-52	Limestone beneath Leylek	*Orbitoides media*	–	Late Maastrichtian
MB10-115	Limestone beneath Ağharman	*Pseudovalvulineria clementiana*	*Rugoglobigerina hexacamerata, Globotruncana falsostuarti, Globotruncanella havanensis, Heterohelix* sp., *Pithonella ovalis*	Late Maastrichtian

the basin. Exposures to the south and northeast of Hekimhan thicken northwards and northwestwards, respectively, towards the inferred basin depocentre. These carbonate rocks are dated as Maastrichtian by an assemblage of benthic foraminifera within bioclastic limestones and also by planktic foraminifera within marls (see Table 4; Fig. 9b). The bioclastic limestones are dominated by fragmentary gastropods, bivalves and echinoderms together with algal rodoliths. Beds range in thickness from 5 to 100 cm and are often laminated, with poorly developed cross lamination. Some coarser grained beds have been partially recrystallised to calcite spar. The calcarenites are interpreted as mostly redeposited, whereas the marls originated as relatively deep-marine sediments.

Calcarenite interbeds become thicker and more numerous upwards relative to hemipelagic marl. Also, the relative abundance of benthic foraminifera (compared to planktic foraminifera) increases up-section, suggesting that the source areas of the calcarenites (around the basin margins) progressively shallowed.

The Hüyük Formation represents shallowing as the sedimentary accommodation space filled. Little syn-sedimentary deformation is observed in contrast to the underlying Hekimhan Formation, which suggests a change to a more stable tectonic setting. The sequence was capped by localised fractured, dissolved and recemented horizons that are interpreted as subaerial palaeokarst.

5.2. Paleocene basin development

Localised deposits of gypsum outcrop in several areas of the Hekimhan Basin, known as the Ağharman Member (see Fig. 3). The gypsum shows wavy, to saw-tooth lamination on a millimetre-scale and also commonly tepee-type and chicken-wire structures, which are suggestive of a sabhka-type origin (Gunatilaka and Mwango, 1987). However, some gypsum horizons are chaotically folded which could be the result of partial dissolution and collapse and, or syn-tectonic deformation. The evaporites are intercalated with thin layers of pale red mudstone (<5 mm thick), which are laterally discontinuous and marked by textures indicating diagenetic redox changes (e.g. Liesegang rings).

The exact stratigraphic position of the evaporites remains poorly constrained in view of limited field exposure. The limestone karst that caps the Hüyük Formation is likely to have been covered by the evaporites, although no contact between these two units is exposed. A Paleocene age for the evaporites has been suggested (Yalcın and Bozkaya, 1996) based on a comparison of $\delta^{34}S$–$\delta^{18}O$ with well-dated ancient samples elsewhere; this age would be in agreement with our field observations.

Our suggested interpretation is that the preceding basin fill was subaerially exposed and karstified. The karst was then repeatedly flooded by seawater, favouring the formation of gypsum in local depressions, either as direct precipitates or as sabhka deposits. A Late Paleocene eustatic sea level rise (Miller et al., 2005) could have periodically flooded the land surface, followed by repeated evaporation under arid conditions.

In some other areas of the Hekimhan Basin (~5 km SSE of Hekimhan) correlative facies of the evaporites comprise red continental mudstones, sandstones and conglomerates, alternating with white lacustrine limestones. The deposition of these sediments was accompanied by the development of a shallow (<5°) basin-wide unconformity, although the precise unconformity surface is rarely exposed.

5.3. Eocene basin development

5.3.1. Sedimentary facies

Eocene sediments are represented by the Akpınar Formation, which varies considerably within the Hekimhan Basin. Microfossil dating shows that this formation ranges from Early to Mid Eocene in age (Ilerdian–Lutetian; Table 5; Fig. 9c–r).

To the southeast of the basin, around Akpınar, the base of the Akpınar Formation is represented by red conglomerates, sandstones and mudstones that are interbedded with white, sandy, unfossiliferous limestones (Fig. 17a). The clasts within the conglomerate are subrounded, up to cobble grade and predominantly composed of unfossiliferous white limestone. The conglomerates and sandstones are typically lenticular, laterally discontinuous and commonly appear to be weakly deformed. This sequence is overlain by an interval (~10 m thick) of undeformed hemipelagic marl with bioclastic limestone (calcarenite) intercalations, followed by massive limestone (~20 m, Fig. 17b). The calcarenites and massive limestones contain abundant *Nummulites* sp. (Table 5; Fig. 9i, j and r), also fragmented bivalves, gastropods and echinoderms.

A similar sequence of red clastic rocks and white limestones is present elsewhere in the basin (i.e. east of Haydaroğlu; Fig. 3). However, the overlying marl and calcarenite sequence is much thicker (up to 100 m) in this area and contains localised basaltic volcanic rocks (Kocaözü Member; see below). Slump folds are also present within the marls in this area.

In contrast, the red clastic sequence is absent to the south of Hekimhan (around Kocaözü; Fig. 3). Marl, calcarenite and, locally, basalt, pass directly into massive Nummulitic limestones, up to 50 m thick. The marls are weakly folded, whereas the limestone interbeds are faulted (Fig. 17c).

The massive limestones near the top of the Akpınar Formation are predominantly recrystallised carbonate. Fossils include *Nummulites* sp. and other benthic foraminifera, together with mollusc and echinoid fragments (Fig. 17d). Above the limestones comes a sequence of silty marls (~40 m thick), interbedded with fine-grained calcarenites (individually 5–20 cm thick). Asymmetrical current ripples are locally present. Organic matter includes fossil leaves (Fig. 17e). The sequence passes into thin (<50 m), localised evaporitic deposits consisting mainly of alabastrine gypsum and gypsiferous marls.

Table 5
Calcareous microfossils identified in limestones of the Eocene Akpınar Formation limestone.

Akpınar Formation (Eocene)				
Samples	Rock type	Benthic Foraminifera	Planktic Foraminifera	Age
MB08-32	Marly limestone	*Idalina sinjarica, Periloculina slovenica, Chrysalidina* aff. *floridana, Spirolina* sp., *Pfendericonus* sp.	–	Late Paleocene
MB08-60	Micrite	–	*Acarinina* sp., *Pseudohastingerina* sp.	Eocene
MB10-38	Nummulitic sandstone	*Nummulites* cf. *Striatus, Assilina* cf. *praespira, Neorotalia vienotti, Assilina* cf. *sphaerogypsina globula*	–	Mid Eocene (Lutetian)
MB10-66	Nummulitic limestone	*Idalina sinjarica, Alveolina* cf. *aragonensis, Chrysalidina* cf. *floridina, Alveolina* cf. *cuspidata, Periloculina* cf. *slovenica, Pfendericonus* sp.	–	Early Eocene (Ilerdian)
MB10-69	Nummulitic calcarenite	*Asterigerina rotula, Neorotalia vienotti, Discocyclina* cf. *scalaris, Assilina* cf. *praespira, Orbitoclypeus* cf. *ramaraoi ramaraoi, Nummulites millecaput, Nummulites* cf. *striatus, Operculina* sp.	*Acarinina bullbrooki, Igorina broedermani, Globigerinatheka* sp., *Subbotina* sp.	Mid Eocene (Lutetian)
MB10-80	Nummulitic limestone	*Nummulites* cf. *minervensis, Alveolina* cf. *aragonesis, Lockhartia haimei, Orbitolites* sp.	*Morozovella* sp., *Chiloguembetina* sp.	Early Eocene (Ilerdian)
MB10-83	Nummulitic limestone	*Orbitolites complanatus, Nummulities* cf. *minervensis, Alveolina* cf. *ellipsoidalis, Alveolina pasticillata, Alveolina (Glomalveolina) levis, Opertorbitolites* cf. *latimarginalis, Idalina sinjarica*	–	Early Eocene (Ilerdian)
MB10-87	Nummulitic limestone	*Alveolina (Glomalveolina) lepidula, Chrysalidina* cf. *floridina, Medocia blayensis, Idalina Sinjarica, Orbitolites* sp.	Indet. planktic foraminifers	Early Eocene (Ilerdian)
MB10-113	Nummulitic limestone	*Nummulites* cf. *striatus, Assilina* cf. *spira, Medocia blayensis, Gyroidinella magna, Neorotalia vienotti, Ranikothalia* sp., *Orbitolites* sp.	*Globigerinatheka* sp.	Mid Eocene (Lutetian)
MB10-114	Nummulitic limestone on top of red facies	*Alveolina (Glomalveolina)* sp., *Orbitolites* sp.	Indet. planktic foraminifers	Latest Paleocene to Mid Eocene
MB10-122	Nummulitic limestone beneath Kocaözü Member	*Alveolina (Glomalveolina) lepidula, Alveolina (glomaveolina) subtilis, Fabularia* cf. *donatae, Orbitolites* sp., *Lockhartia* sp.	–	Early Eocene (Ilerdian)

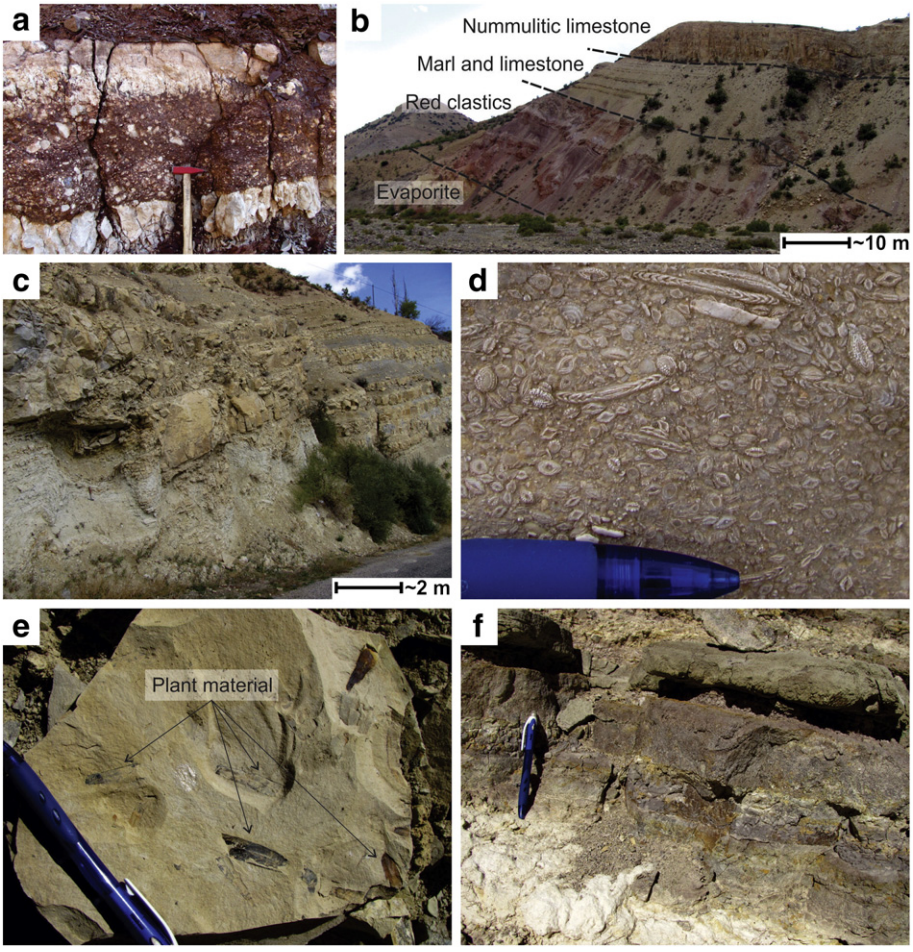

Fig. 17. Photographs showing (a) red conglomerate with limestone clasts interbedded with white unfossiliferous limestone beds; (b) lower part of the Akpınar Formation from the southeast of the basin; (c) folded and sheared marls overlain by massive, block faulted limestone beds; (d) nummulites sp. etchings on a weathered surface of recrystallised limestone; (e) plant debris from the upper part of the Akpınar Formation; and (f) volcaniclastic sandstone deposits from the upper part of the Akpınar Formation. Hammer for scale in (a); pencil for scale in (d)–(f).

Volcaniclastic sandstone and light brown, very fine-grained tuff are locally present within the upper part of the Akpınar Formation. The sandstones are dark-grey to dark-brown, predominantly medium-grained, relatively structureless and mainly composed of sub-angular mafic mineral grains (Fig. 17f).

To the south of the main basin area, a thin (~40 m thick) sequence of marls passes upwards into massive *Nummulites*-bearing calcarenite and limestone (>100 m thick), exposed in vast canyons (Fig. 3).

In western areas of the basin the sedimentary rocks are characterised by a generally thinner sequence (<50 m). Marls there are intruded by columnar-jointed dykes (up to 5 m thick), which form part of the Leylek Formation (see below). The limestones contain abundant echinoid spines and isolated, in situ, colonial corals.

The shallow-marine Akpınar Formation accumulated in a tectonically active setting as indicated by localised slump folding and basic volcanism (see below). The basin emerged towards the end of the Eocene, probably reflecting one or a combination of sediment infill, eustatic sea level fall (Miller et al., 2005), or regional uplift.

5.3.2. Volcanogenic intercalations

Basaltic rocks, termed the Kocaözü Member (Fig. 5), interrupt the Early–Middle Eocene marls of the Akpınar Formation in parts of the basin (e.g. to the south and SE of Kocaözü; Fig. 3). Plagioclase- and clinopyroxene-phyric basalt is typically pillowed, with peperite structures (e.g. 'load balls') developed along the contact between marls and overlying volcanic rocks. The basalts are locally overlain by a thin sequence (<2 m thick) of dark-grey volcaniclastic conglomerate. The volcanogenic rocks are both underlain and overlain by *Nummulites*-bearing carbonates.

Six samples of basaltic rocks from the Kocaözü Member were chemically analysed (see Table 2). The results are plotted on a volcanic rock classification diagram (Fig. 11) and as a MORB-normalised spider diagram (Fig. 18), showing that the rocks are basalts and basaltic andesites, of generally within-plate type (although basaltic andesites are unsuitable for tectonic discrimination).

Within the upper part of the Akpınar Formation, especially within the western part of the Hekimhan Basin (Fig. 3), there are also localised intercalations of andesite and dacite, known as the Leylek Member (Fig. 5). When analysed (see Table 2), these rocks plot in the andesite, trachy-andesite and rhyolite fields on the total alkali versus silica (TAS) volcanic classification diagram (Fig. 11). $^{40}Ar/^{39}Ar$ K-feldspar geochronology has yielded an age of 34.4 ±1.1 Ma (Kuşcu et al., 2007), i.e. close to the Eocene–Oligocene boundary, which is consistent with the observation that the sedimentary succession continues up into the Mid–Late Eocene (Lutetian). The fractionated silicic rocks are interpreted as syn-collisional to post-collisional volcanism, as documented elsewhere throughout the region (Keskin et al., 2008; Kuşcu et al., 2007, 2010).

5.4. Post-Eocene facies

As a continuously developing regional depocentre, the Hekimhan Basin is considered to have ended prior to the Oligocene. However, the younger sediments within the geographic confines of the basin shed light on sea level change and the timing of regional uplift. Unconformably overlying non-marine sediments, of inferred Oligocene age, are mainly red fluvial sandstone and conglomerates (Kamatlar Formation) (Fig. 5). These sediments were derived from all of the formations of the underlying Hekimhan Basin showing that the basin was dissected and exposed to erosion by this time.

Continental sedimentation was followed by a localised marine transgression, which probably resulted from a eustatic sea level rise (e.g. Miller et al., 2005). The transgression resulted in the deposition of thin (<50 m), shallow-marine facies of Middle Miocene age (Gürer, 1994). In particular, bioclastic limestones exhibit south-westward-prograding Gilbert-type foresets (Boyralı Formation; Fig. 5). The presence of the Middle Miocene shallow-marine sediments shows that post-collisional regional uplift was postponed until after this time.

The northern part of the Hekimhan Basin is capped by thick sequences (up to 1000 m) of Middle Miocene subaerial lava flows, together with volcaniclastic sediments (Yamadağ Formation; Fig. 5) (Gürsoy et al., 2011). Post-collisional volcanics of similar age are widespread throughout eastern Anatolia (Arger et al., 2000; Demir et al., 2009; Ekici et al., 2009).

5.5. Structural development of the Hekimhan Basin

The Hekimhan Basin is cut by a range of extensional, compressional and strike-slip related structures that shed additional light on the tectonic development of this sedimentary–magmatic basin.

Normal faulting is observed in Maastrichtian-aged rocks, especially the Karadere and Hekimhan Formations. The majority of these faults display metre-scale offsets without observable kinematic evidence of the direction of movement. However, where observable, offsets are typically 20 cm vertically, with fault cores (damage zones) <5 cm wide. When the measured faults are plotted on a stereonet (Fig. 19a) the

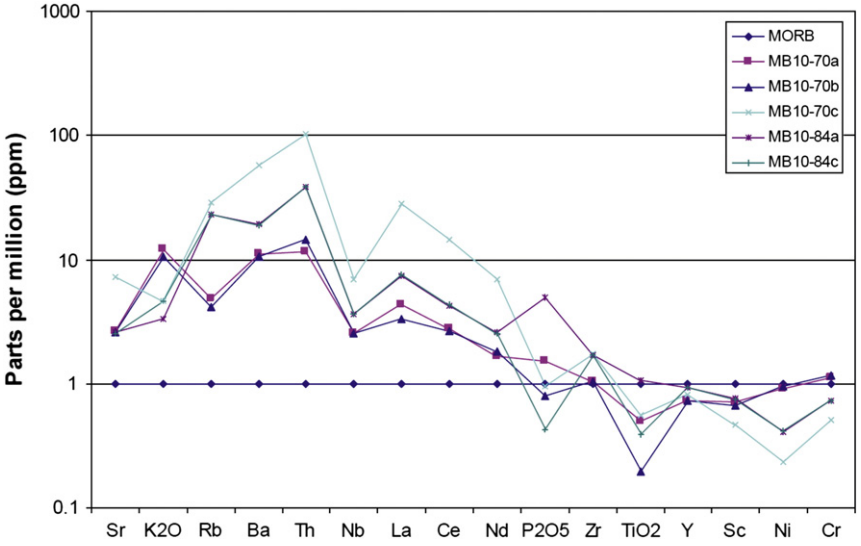

Fig. 18. Mid-ocean ridge basalt (MORB)-normalised spider diagrams for the Eocene extrusive rocks (Kocaözü Member). Normalising values from Pearce (1982) and Saunders and Tarney (1984). See text for discussion.

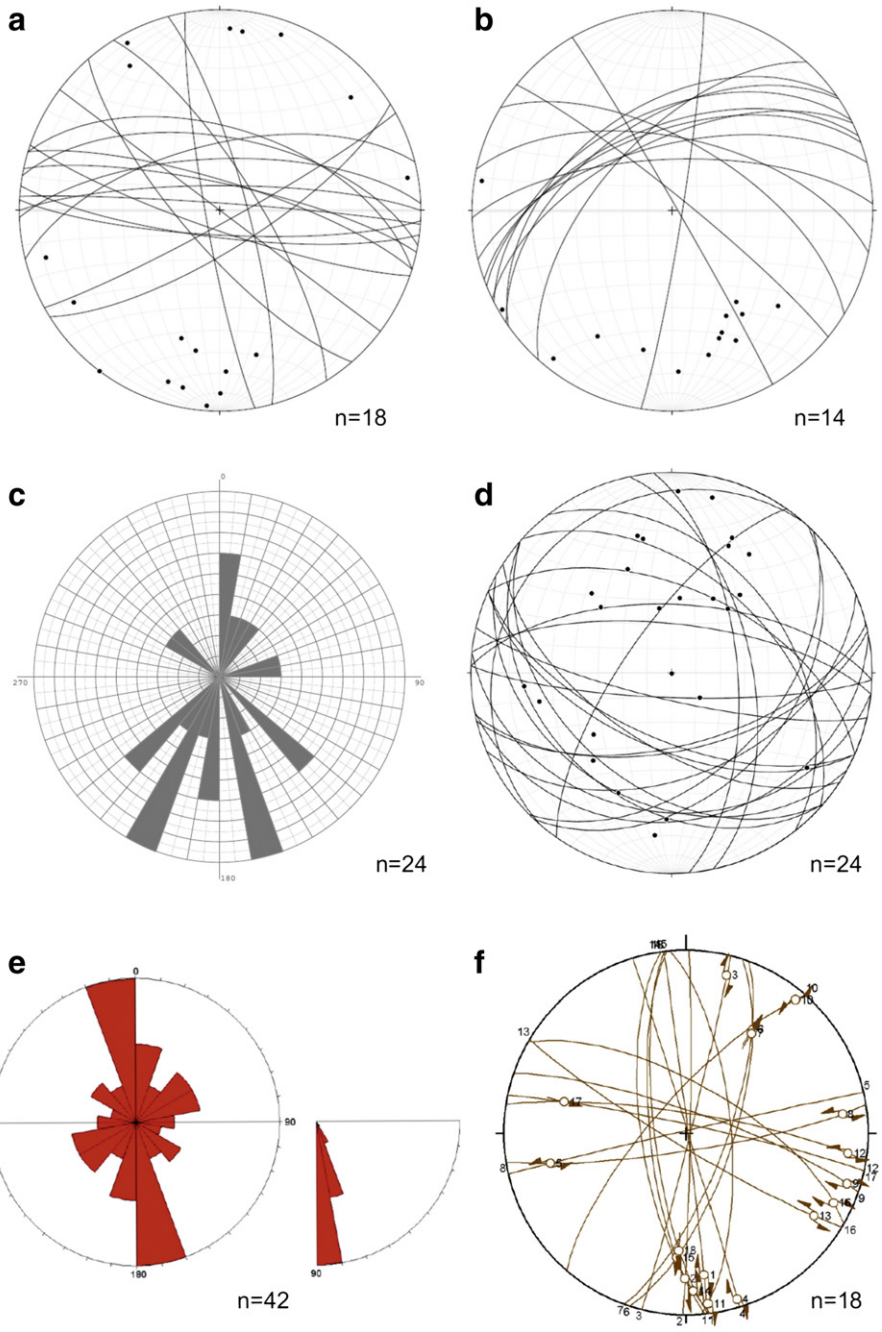

Fig. 19. Equal-area stereonets showing (a) great circles and poles to planes of extensional fault planes measured within the Maastrichtian Karadere and Hekimhan Formations ($n = 18$); (b) great circles and poles to planes of extensional fault zones measured within the Eocene Akpınar Formation ($n = 14$); (c) rose diagram showing the dip directions of all of the measured reverse faults in the Hekimhan Basin; (d) equal-area stereonet showing great circles and poles to planes of reverse fault planes observed within the Hekimhan Basin ($n = 24$); (e) bidirectional rose diagram of all strike-slip faults; and (f) Angelier plot showing great circles of strike-slip fault planes with associated kinematic features (slickensides).

majority are seen to be orientated E–W, with displacements either to the north or to the south.

Few extensional faults were observed within the Maastrichtian volcanogenic rocks (Hasançelebi Formation). However, extensional faults were rarely observed cutting the highest levels of the Maastrichtian succession.

Extensional structures in the Eocene sequences are limited to a series of small normal faults, as observed in the east and south of the basin. These faults are generally <5 m long in outcrop, with fault cores <2 cm wide and vertical offsets <10 cm. Most of these faults are orientated E–W and dip towards the north (Fig. 19b).

Compressional faults are widespread throughout the Maastrichtian, up to and including the Oligocene rocks but are absent from the Miocene rocks. When plotted on a rose diagram (Fig. 19c), measured reverse faults indicate a strong N–S orientation of dip directions. An E–W orientation is confirmed when the faults are plotted on a stereonet (Fig. 19d). There is a strong clustering of southerly inclined faults, whereas other faults are generally inclined to the north, i.e. indicative of ~N–S shortening.

The Hekimhan Basin and adjacent areas are cut by numerous strike-slip faults. These are mostly exposed in valleys and canyons making it difficult to evaluate lateral offsets. Only one slip surface is typically preserved on each fault scarps such that the original fault cores are rarely preserved. Forty-two strike-slip fault planes were recorded from the Hekimhan Basin (Fig. 19e). Of these, 20 display slickensides with kinematic orientations sufficient to delineate offset direction (i.e. sinistral

versus. dextral). Both sinistral and dextral faults appear to be equally abundant in the recorded data set (Fig. 19f).

6. Discussion

6.1. Hekimhan Basin development

The initiation of the Hekimhan Basin immediately followed the emplacement of accretionary mélange and ophiolitic rocks onto the Tauride continental margin. The ophiolite-related mélange, of both tectonic and sedimentary origin, was emplaced southwards during the Maastrichtian (Fig. 20a). The emplacement was facilitated by regional subsidence of the carbonate platform to form a foredeep, as documented in an adjacent area (e.g. Gürün area to the northwest; Robertson et al., 2013b). The tectonic and sedimentary mélanges beneath the Hekimhan Basin reflect subaqueous gravitational emplacement. Immediately after the emplacement the foredeep emerged resulting in erosion and then the deposition of the red fluvial clastic sediments (Karadere Formation; Fig. 20b). The emergence was possibly facilitated by regional flexural relaxation soon after the inferred subduction zone-continental margin collision ended. A marine transgression initiated the construction of elongate rudist mounds on topographic highs that are likely to have been fluvially and structurally influenced. The basin then deepened, as indicated by syn-depositional facies and structural evidence (Fig. 20c). The subsidence was accompanied by eruption of thick basaltic lavas of alkaline, within-plate type that were locally reworked to produce volcaniclastic material (Fig. 20d). Interbedded mudrocks and fine-grained sandstones were derived from surrounding continental crust and the emplaced ophiolitic rocks. The Late Cretaceous alkaline magmatism as a whole included the intrusion of syenite, although this may have pre-dated the basaltic lava eruption. After the extensional phase ended the by then relatively deep-water basin gradually filled until it broke surface by latest Maastrichtian to Early Paleocene time (Fig. 20e). The basin remained close to sea level during the Paleocene during which time non-marine clastic, lacustrine and probably also, evaporitic sediments accumulated (Fig. 20f).

The Hekimhan Basin experienced a second phase of marine transgression during the Early Eocene (Fig. 20g), followed by further, alkaline within-plate-type volcanism (Fig. 20h). The basin then shallowed-upwards to a second regional unconformity, prior to the Oligocene (Fig. 20i). Sedimentation in the Hekimhan Basin ended during the Mid–Late Eocene (Late Lutetian). Shallow-marine sediments and evaporites indicate progressive shallowing and isolation of the basin, followed by eventual emergence. The compression affecting the basin mostly post-dated the Late Eocene sedimentation but preceded the localised deposition of the Mid-Miocene transgressive limestones (Boyralı Formation; Fig. 20j).

The strike-slip faulting affecting the Hekimhan Basin largely post-dated the deposition of the sub-horizontal Mid-Miocene shallow-water limestones. The absence of any preferred offset direction of the measured

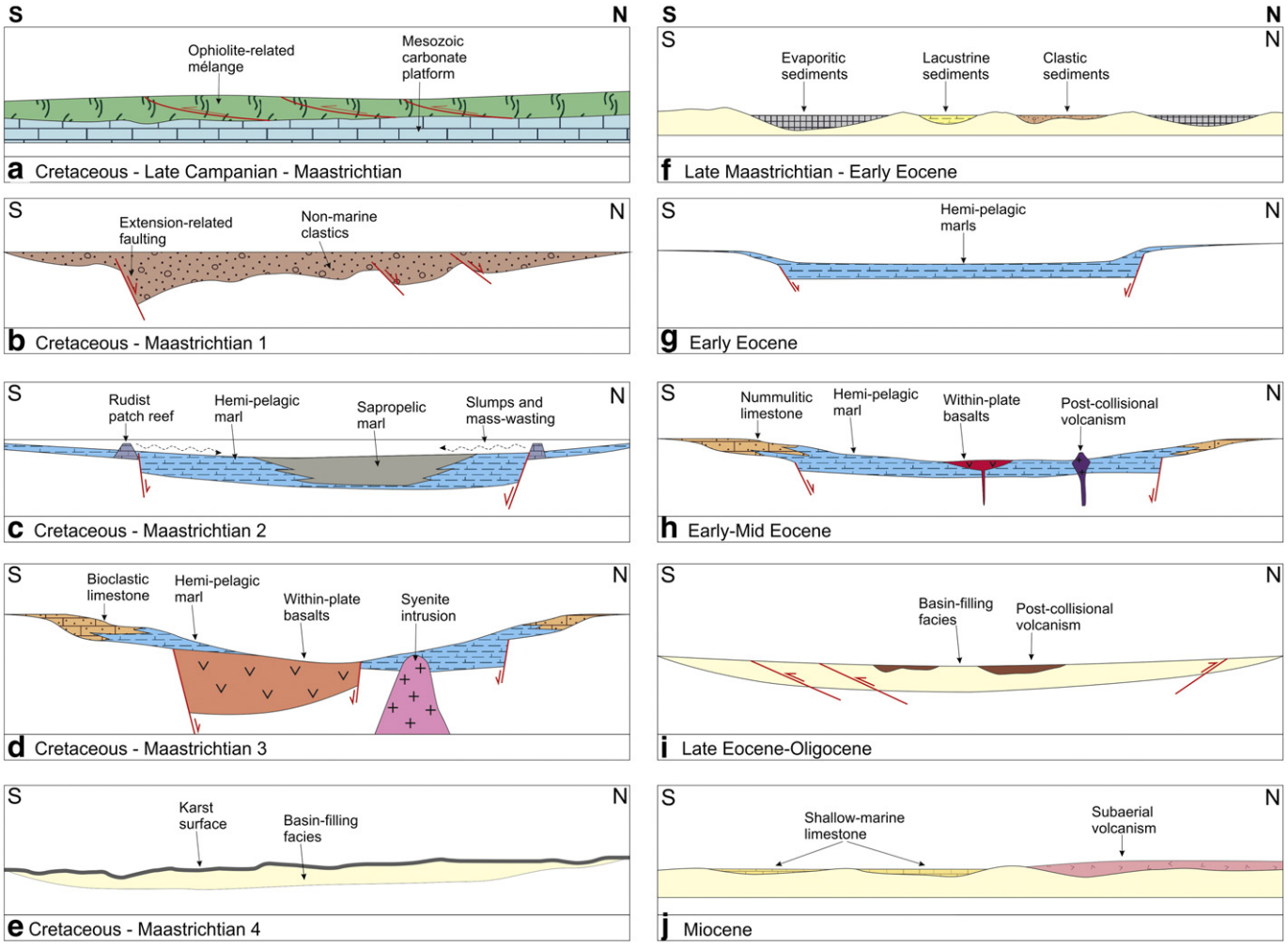

Fig. 20. Summary of Hekimhan Basin evolution. (a) Precursor emplacement of oceanic rocks. (b) Early-stage extensional faulting. (c) Basin subsidence. (d) Alkaline magmatism. (e) Basin emergence. (f) Variable non-marine to evaporitic deposition. (g) Renewed basin subsidence. (h) Further alkaline magmatism. (i) Basin compression and non-marine deposition. (j) Post-basinal marine transgression and subaerial volcanism. Note: for simplicity only features relating to each individual time slice are indicated.

neotectonic strike-slip faults is surprising. Studies of Pliocene–Recent strike-slip faulting further south indicate almost exclusively left-lateral displacement (Duman and Emre, 2013). However, kinematic analysis of the area to the northeast of the Hekimhan Basin (Gürün area) reveals similar evidence of both right-lateral and left-lateral strike-slip. The right-lateral strike-slip may have pre-dated the Pliocene–Recent left-lateral strike slip that was related to the regional westward tectonic escape of Anatolia (see Robertson et al., 2013b). Thus, the measured strike-slip faults in the Hekimhan Basin could record two different timings of displacement with differing directions of motion.

Regional uplift to form the Anatolian plateau took place after the Mid-Miocene onwards generally related to Arabia-Eurasia collision (e.g. Ballato et al., 2010; Schildgen et al., 2012).

6.2. Supra-ophiolite basins to the east and west

Ophiolites and accretionary mélange were emplaced along the entire length of Anatolia from the Aegean to Iran during latest Cretaceous time. This prompts a quest for comparable supra-ophiolite basins to the west or east. Most comparable and nearest to the Hekimhan Basin is the Darende Basin ~60 km to the southwest (Fig. 1b). The Darende Basin exhibits emplacement of accretionary mélange and ophiolitic rocks over the regional Tauride platform, including larger thrust slices of ophiolitic rocks than those beneath the Hekimhan Basin. Both basins show evidence of a short-lived non-marine setting, followed by a Maastrichtian marine transgression and shallow-water carbonate deposition. However, in contrast to the Hekimhan Basin, the Maastrichtian marine sedimentation remained relatively thin, without associated volcanism in the Darende Basin. Syn-sedimentary faulting is locally observed near the southwestern basin margin. The lack of subsidence and the absence of Maastrichtian volcanism in the Darende Basin can be explained by lesser crustal extension compared to the Hekimhan Basin.

Paleocene sediments are absent from the Darende basin, whereas relatively thin non-marine and evaporitic sediments accumulated in the Hekimhan Basin. However, only a small difference in elevation between the two basins could explain these facies contrasts. Both basins show evidence of renewed marine transgression during the Early Eocene, followed by deepening and subaqueous volcanism of within-plate type. Both basins shallowed and became emergent, associated with regional post-suture compression.

The Hekimhan Basin can also be compared with the Ülükışla Basin, ~300 km to the west. The Ülükışla Basin is bounded by the Tauride carbonate platform to the south and by the Niğde–Kırşehir continental massif to the north (Fig. 1b). Ophiolites and accretionary mélange were again emplaced southwards over the Tauride platform. However, in this case the former northern edge of the Tauride platform was detached and emplaced southwards during the latest Cretaceous to create the Bolkar Nappe. The more proximal (southerly) part of the Tauride platform subducted and underwent HP/LT metamorphism, typical of the Anatolide belt (Pourteau et al., 2010; Robertson et al., 2009). The HP/LT rocks rapidly exhumed and were locally reworked in a short lived non-marine setting, followed by marine transgression and the establishment of shallow-marine carbonate deposition during the Maastrichtian (Robertson et al., 2009). In response to crustal extension (or possible transtension), the Ülükışla Basin then subsided rapidly, triggering the accumulation of mixed terrigenous-carbonate sediments as gravity flows (turbidites and debris-flow deposits). This was accompanied by (and also followed by) extensive extrusive and intrusive magmatism of within-plate type, similar to the Hekimhan Basin (Clark and Robertson, 2002, 2005). However, peak magmatism was delayed until the Paleocene–Early Eocene in the Ülükışla Basin. The Ülükışla Basin shallowed upwards during the Mid–Late Eocene, culminating in local evaporitic deposition, in parallel to the Hekimhan and Darende basins. Despite the general similarities, the Hekimhan Basin is underlain by unmetamorphosed Mesozoic Tauride carbonate platform rocks, whereas the Ülükışla Basin is floored by exhumed metamorphic rocks of the Anatolide HP-LT belt (Pourteau et al., 2010; Robertson et al., 2009). The probable explanation of this difference is that the Hekimhan Basin developed on the detached over-riding plate whereas the Ülükışla Basin formed on the exhumed down-going plate (relatively further south).

In contrast with both the Ülükışla and Darende Basins, the Hekimhan Basin underwent intense thrusting and folding, prior to the accumulation of Oligocene non-marine sediments. This difference in the structural intensity can be explained by the indentation of the Nığde–Kırşehir continental block with the Tauride continent during late-stage collision, and/or post-collisional suture tightening.

To the east of the Hekimhan Basin, the southern margin of the regionally extensive Sivas Basin (Fig. 1b) shows evidence of Late Cretaceous subsidence and extensional faulting (Guezou et al., 1996; Poisson et al., l996; Kavak et al., 1997; A. Poisson, pers. com., 2012).

To the west of the Ülükışla Basin, the emplaced ophiolites are mainly covered by relatively thin deposits of shelf-depth, Nummulitic Eocene limestones and marls (e.g. in the Konya area), without any recurrence of the Maastrichtian depocentres further east.

6.3. Comparable supra-ophiolite basins elsewhere

Comparable supra-ophiolite basins are found associated with another suture zone in Turkey, namely the Southern Neotethyan suture zone, which is located to the south of the Tauride carbonate platform in SE Turkey (Fig. 1b). Supra-subduction zone-type ophiolites and accretionary mélange in this region were emplaced southwards onto the Arabian continental margin during latest Cretaceous time in response to regional collision of a subduction zone with the Arabian margin (Robertson, 2002; Yılmaz et al., 1993). The associated sedimentary rocks show similarities with the Hekimhan Basin and other Tauride supra-ophiolite basins, as summarised above. Ophiolites and mélange emplacement was followed, first by localised accumulation of non-marine sediments, and then by a marine transgression that ushered in shallow-marine carbonate deposition (including rudist reefs) during the Maastrichtian. The basin deepened upwards during the Paleocene, with hemi-pelagic marl deposition, followed by shallowing upwards and Nummulitic carbonate deposition during the Eocene. There was then a transition upwards to terrigenous turbidites (Lice Formation) that accumulated in a foreland basin setting, prior to overthrusting by Tauride-derived thrust sheets.

The eastward extension of the same southerly belt of emplaced ophiolites far to the east, in Oman, offers a further interesting comparison. Ophiolites, accretionary mélange and continental margin units were emplaced onto the bordering Arabian continent during latest Cretaceous time (Glennie et al., 1990; Robertson and Searle, 1990). In this case an ocean still persisted to the east, within the Gulf of Makran. The emplacement of allochthonous units was followed by short-lived emergence and localised fluvial deposition (e.g. in the United Arab Emirates in the north), similar to the Hekimhan Basin. A marine transgression resulted in the local development of Maastrichtian rudist reefs (Shelton, 1990). Extensionally controlled basins opened during the Maastrichtian in which gravity flows were emplaced and alkaline volcanic rocks erupted (Filbrandt et al., 1990).

The similarities of the Oman and Tauride examples, especially the Hekimhan Basin, indicate that many common features, notably extension, subsidence and alkaline volcanism can occur independently of continental collision, which in all of the areas summarised did not take place until many millions of years later. The Hekimhan, Darende and Ülükışla Basins mainly developed during the Maastrichtian to Early–Mid Eocene, prior to the final suturing of the Tethyan Ocean to the north, which was complete by late Mid-Eocene (Bartonian; ~45 Ma).

Comparable supra-ophiolite basins are also associated with the Jurassic Balkan ophiolites. Notably, in Greek Macedonia and the neighbouring Republic of Macedonia, ophiolites of supra-subduction zone type were emplaced generally southwards onto the Pelagonian continent. The ophiolitic rocks were then subaerially exposed, eroded

and transgressed by shallow-marine siliciclastic and carbonate sediments during the latest Jurassic (Tithonian). The basin subsided under an inferred extensional control, associated with the further deposition of mixed siliciclastic–carbonate gravity deposits (turbidites and mass-flow deposits). For a time during the Mid Cretaceous the basin became magmatically active with the eruption of pillow basalts. The basin terminated during the latest Cretaceous with regional thrusting related to the final closure of the Vardar Ocean to the northeast (see Robertson et al., 2013c and references therein).

Additional examples of comparable supra-ophiolite basins no doubt exist, for example associated with the Late Palaeozoic closure of the Iapetus Ocean in North America.

6.4. Alternative tectonic models for supra-ophiolite basin development

Taken together, the similarities of the supra-ophiolite basins of different ages and different location suggest that a common driving mechanism is likely to be involved. Common to all of the supra-ophiolite basins is an extensional control related to a pre-collisional setting, as shown in Fig. 21a and b. For the Taurides–Anatolides, specifically to the west of the study area, there is additional evidence of regional crustal extension during latest Cretaceous–Paleocene time. The HP-LT metamorphic rocks of the Anatolides were exhumed during this time period, in a setting of inferred crustal extension, well prior to continental collision (see Robertson et al., 2009 for discussion and literature).

For the Hekimhan Basin, the first, and dominant, phase of basin development involved drastic subsidence and related alkaline volcanism during the Maastrichtian. In principle, the Maastrichtian subsidence of the Hekimhan Basin could be explained by several different settings including rifting and regional flexural loading. There is only limited direct evidence of coeval extensional faulting, although such structures would predominate in the substratum of the basin, which is not exposed. In addition, where present, extensional faults could have been obscured by later-stage compressional and strike-slip faults. However, taken with the evidence of alkaline magmatism and the regional setting (which includes extensional exhumation of Anatolide HP-LT metamorphic rocks) we infer that an extensional setting is applicable to the Hekimhan Basin during the Maastrichtian.

An obvious option is back-arc rifting related to northward subduction of Neotethys to the south. Subduction is known to have taken place during Late Cretaceous time, as summarised in the introduction to the paper. The southern part of the Tauride-related Malatya–Keban platform was intruded by Late Cretaceous granitoid rocks (Parlak et al., 2013a; Yazgan and Chessex, 1991) to the south of the area studied. This magmatism relates to northward subduction of the Southern Neotethys (Yılmaz, 1993; Robertson, 2004; Robertson et al., 2006, 2009; Parlak et al., 2013b).

On the other hand, back-arc rifting is unlikely to be the primary cause of the Maastrichtian subsidence and basaltic volcanism in the Hekhiman Basin. Back-arc basins typically develop by rifting of an already developed magmatic arc (e.g. modern Mariana and Tonga arcs; Karig et al., 1975; Taylor, 1992), which is, however, absent from within or around the Hekimhan Basin. In addition, there is no evidence of arc magmatism affecting the northern part of the Mesozoic Tauride carbonate platform in the surrounding region during the Late Cretaceous, for example, associated with the subjacent Mesozoic Tauride carbonate platform rocks (Robertson et al., 2013b), or the Munzur Massif further northeast (MTA, 2002). Several of the other comparable supra-subduction zone basins (e.g. latest Cretaceous of Oman) are not explicable by back-arc rifting.

The alternative, which we favour, is that the regional extension during the Maastrichtian resulted from the gravitational pull of the oceanic plate, which was still subducting northward beneath the Eurasian margin (in the Pontides) during late Cretaceous–Palaeocene time (Fig. 21a and b). The northward subduction of Tethyan oceanic crust continued after latest Cretaceous ophiolite emplacement until collision during Late Palaeocene–Early Eocene time. This oceanic crust could comprise relicts of the Inner Tauride Ocean and/or the İzmir–Ankara–Erzincan ocean.

The interpretation of the Early–Middle Eocene basalts and basaltic andesites (Kocaözü Member) and the Eocene–Oligocene andesite and dacites (Leylek Member) is again debateable. The former (Kocaözü Member) erupted during the latest stages of closure of Neotethys (in the Pontides), while the later (Leylek Member) post-dated the ocean suturing. The Early–Middle Eocene basalts and basaltic andesites are broadly of extensional within-plate type.

Back-arc rifting is an option for the Eocene tectonic setting since there is evidence of Eocene northward subduction to the south of the Hekhiman Basin, known as the Maden back-arc basin, which developed associated with the Pütürge and Bitlis continental units (Yazgan and Chessex, 1991; Yılmaz, 1993; Robertson et al., 1996; Karaoğlan et al., 2013; see Fig. 2a and b). However, two factors question this possibility. First, the fractionated, alkaline Early–Mid Eocene volcanics of the Hekimhan Basin contrast with the coeval basaltic, tholeiitic, subduction-influenced basalts of the Maden back-arc basin (Robertson et al., 2006; Yiğitbaş and Yılmaz, 1996). Secondly, the Malatya Metamorphic unit to the south of the Hekhiman Basin is transgressed by Eocene shallow-water carbonates without evidence of strong subsidence or coeval volcanism (Perınçek and Kozlu, 1984; Robertson et al., 2006; Bedi et al., 2012). The Eocene extension-related volcanism in the Hekhiman Basin may, therefore, be too far north from the Eocene Maden back-arc basin to be directly related.

The Eocene marine transgression and within-plate volcanism could alternatively relate to loading of the regional foreland (made up of Tauride crust) during continental collision (in the Pontides and Caucasus). The continents bordering the relict Neotethys to the north (i.e. oceanic crust surviving after Late Cretaceous) were in the process of progressive collision during Late Paleocene–Early Eocene (Okay and Şahintürk, 1997; Sosson et al., 2010; Robertson et al., 2014; see Fig. 21c). Foreland basins are not normally volcanically active. However, several foreland basins, including those associated with ophiolite emplacement (e.g. in Oman and Greece), are known to be associated with intra-plate-type volcanism (e.g. Robertson, 2006). We infer that the intensifying collision resulted in flexural subsidence, deformation, fragmentation and magmatism within the Tauride foreland, including the Hekimhan Basin as continental collision intensified.

Collision was complete across central and eastern Anatolia by late Middle Eocene time (see Introduction and references cited there) and thus the latest Eocene intermediate-silicic volcanics (Leylek Member) can be attributed to post-collisional magmatism.

Finally, it should be noted that the whole region was to some extent kinematically linked. Continental collision in the north (in the Pontides) can be seen as the trigger of accelerated subduction of the Southern Neotethys further south (see Robertson et al., 2013a).

7. Conclusions

- The Hekimhan Basin exemplifies a supra-ophiolite basin, an important class of sedimentary–magmatic basin, which has previously received little attention.
- A pre-requisite for the formation of a supra-ophiolite basin, such as the Hekimhan Basin, is that oceanic crust in the form of ophiolites (typically formed in a supra-subduction zone setting) or ophiolite-related mélange was emplaced over an adjacent passive continental margin. Crucially, the ocean basin still remained partially open allowing a basin to form above the emplaced oceanic rocks long prior to continental collision.
- After Late Cretaceous emplacement, which was subaqueous, the ophiolitic rocks and mélange associated with the Hekimhan Basin rapidly emerged, possibly in response to flexural relaxation. This triggered erosion and deposition of non-marine, mostly fluvial, sediments (e.g. braided stream deposits).
- Soon afterwards, within the Maastrichtian, the Hekimhan Basin was

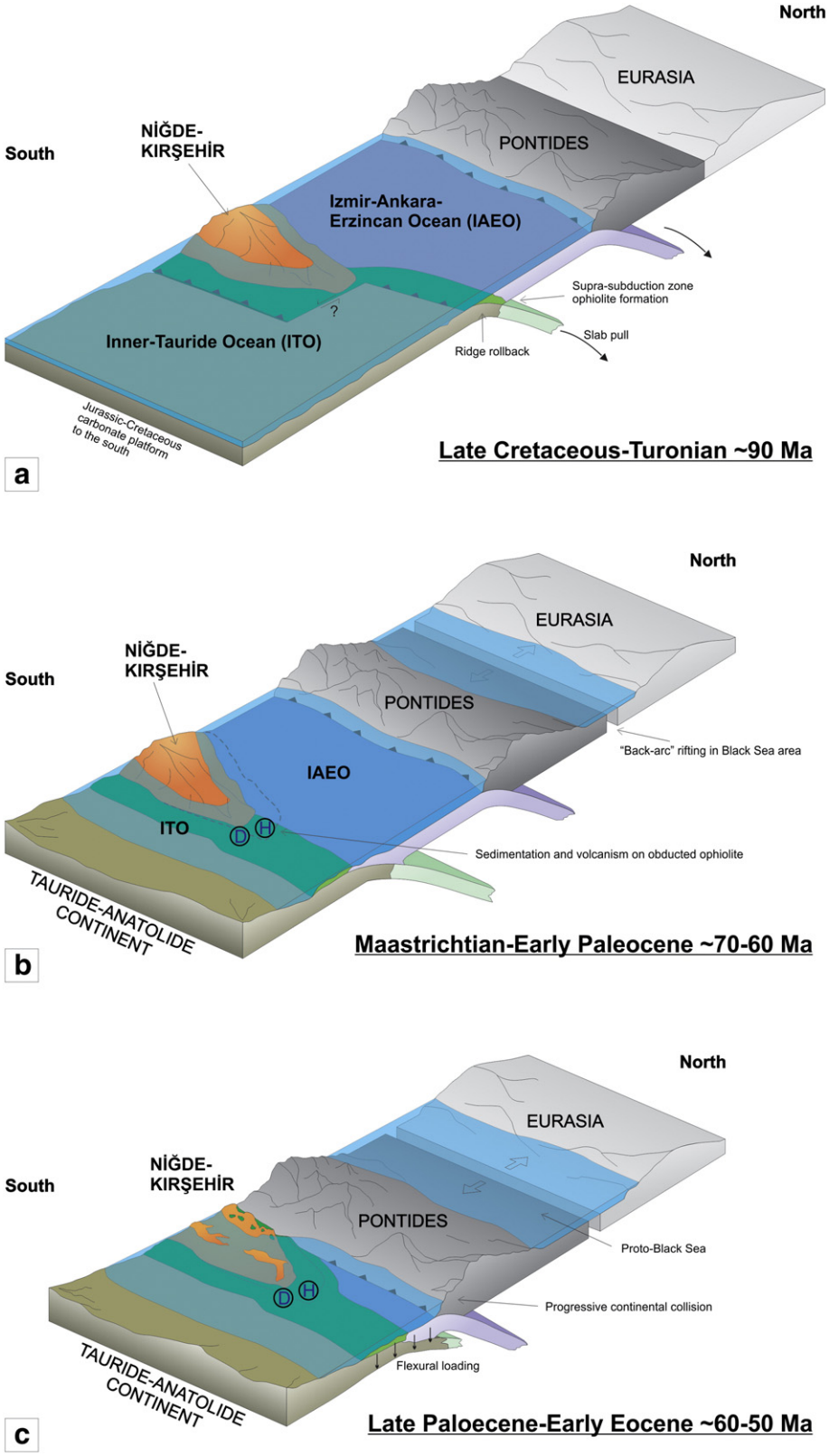

Fig. 21. Plate tectonic reconstructions of central Anatolia based on an integration of available regional data. (a) Late Cretaceous (Turonian) ~90 Ma. Two ocean basins are shown subducting northwards, separated in the west by the Niğde–Kırşehir microcontinent. (b) Late Cretaceous (Maastrichtian) ~65 Ma. Both oceans are shown as subducting northwards. Oceanic crust (ophiolites and accretionary melanges) are emplaced over the leading edge of the Tauride continent. The positions of the future Hekimhan Basin (H) and the Darende Basin (D) are indicated. (c) Early Eocene ~55 Ma. The ocean basin in the north is partially closed. Closure was completed by the Late Middle Eocene (Bartonian) ~45 Ma.

transgressed by shallow seas, ushering in localised rudist reef formation and marginal carbonate platform/slope deposition.

— Basin deepening resulted from crustal extension, in turn triggering gravity-sediment deposition that was mostly bioclastic in the Hekimhan Basin.

— The extension was accompanied by magmatism (both extrusive and

intrusive) of alkaline, within-plate type in the Hekimhan Basin and several other comparable basins (e.g. Ülükışla Basin).
- After the Maastrichtian extensional phase the Hekimhan Basin shallowed upwards under relatively quiescent tectonic conditions.
- During the Paleocene, sedimentation in the Hekimhan Basin was restricted to thin continental and lacustrine deposits, coupled with local accumulation of marine evaporites.
- A Palaeocene low-angle regional unconformity within the Hekimhan Basin is likely to be a response to the initial stages of continental collision to the north (in the Pontides).
- Early–Mid Eocene was characterised by marine transgression, renewed subsidence and further alkaline, within-plate volcanism in the Hekimhan Basin. The likely cause was flexural subsidence related to on-going continental collision to the north and the break-up of the foreland as continental collision intensified. A less likely explanation is back-arc rifting related to opening of the Eocene Maden back-arc basin to the south (in response to northward subduction).
- Late Eocene–Oligocene N–S thrusting and folding of the Hekimhan Basin resulted from post-collisional suture zone tightening.
- Uplift of the Hekimhan Basin took place after a localised Mid-Miocene marine transgression.
- The Hekhiman Basin shows significant similarities with the Darende and Ülükışla basins to the west and with the southern part of the Sivas basin to the east. Comparable supra-ophiolite basins exist elsewhere (e.g. Balkan Tethys, Oman Tethys, and North American Iapetus), confirming the global importance of this class of basin.
- The preferred overall tectonic model envisages extension related to slab-pull to the north during the Maastrichtian, followed by subsidence, magmatism and compression during the Eocene related to progressive continental collision.

We would like to thank Ulvi Can Ünlügenç, Stephen Vincent and Süleyman Karahan for logistical help and discussions in the field. The manuscript benefitted from useful reviews from Yalçın Ersoy and an anonymous reviewer.

Appendix A. Supplementary data

Supplementary data to this article can be found online at http://dx.doi.org/10.1016/j.tecto.2014.05.039.

References

Alpaslan, M., Boztuğ, D., Frei, R., Temel, A., Kurt, M.A., 2006. Geochemical and Pb–Sr–Nd isotopic composition of the ultrapotassic volcanic rocks from the extension related Çamardı–Ulukışla basin, Niğde Province, Central Anatolia, Turkey. J. Asian Earth Sci. 27, 613–627.

Arger, J., Mitchell, J., Westaway, R.W.C., 2000. Neogene and Quaternary volcanism of southeastern Turkey. In: Bozkurt, E., Winchester, J.A., Piper, J.D.A. (Eds.), Tectonics and Magmatism in Turkey and the Surrounding Area. Geological Society, London, Special Publications, 173, pp. 459–487.

Ayan, T. 1961, Detailed geology and petroleum potential of the Hekimhan–Ebreme region (north of Malatya). MTA Rep., 4186 (unpublished), Ankara [in Turkish].

Baier, J., Audétat, A., Keppler, H., 2008. The origin of the negative niobium tantalum anomaly in subduction zone magmas. Earth Planet. Sci. Lett. 267, 290–300.

Ballato, P., Uba, C.E., Landgraf, A., Strecker, M.R., Sudo, M., Stockli, D.F., Friedrich, A., Tabatabaei, S.H., 2010. Arabia-Eurasia continental collision: insights from late Tertiary foreland-basin evolution in the Alborz Mountains, northern Iran. Geol. Soc. Am. Bull. B30091.1.

Bedi, Y., Yusufoğlu, H., Usta, D., Okoyocu, C., 2012. The presence of the Alada and Yahyalı Nappes in the Eastern Taurides (Afşin–Malatya) and their tectonostratigraphic characteristics. In: Yalçın, M.N., Çorbacıoğu, H., Aksu, Ö., Bozdoğn, N. (Eds.), Paleozoic of Northern Gondwana and it Petroleum Potential. Extended Abstracts. Turkish Association of Petroleum Geologists, Special Publications, 6, pp. 24–25.

Booth, M.G., Robertson, A.H.F., Tasli, K., Inan, N., Ünlügenç, U.C., Vincent, S., 2013. Two-stage development of the Late Cretaceous to Late Eocene Darende Basin: implications for closure of Neotethys in central eastern Anatolia (Turkey). In: Robertson, A.H.F., Parlak, O., Ünlügenç, U.C. (Eds.), Geological Development of Anatolia and the Easternmost Mediterranean Region. Geological Society, London, Special Publication, 372, pp. 385–419.

Çaglar, M., Önal, M., 2009. Systematic palaeontology, biostratigraphy, palaeobiogeography of Loftusia (foraminifera) and Rudist assemblages in a regressive sequence in the Hekimhan–Malatya area (Eastern Anatolia) Turkey. J. Geol. Soc. India 74, 329–342.

Cann, J., Gillis, K., 2004. Hydrothermal insights from the Troodos ophiolite, Cyprus. In: Davies, E.E., Elderfield, H. (Eds.), Hydrogeology of the Oceanic Lithosphere. Cambridge University Press, pp. 274–310.

Clark, M., Robertson, A.H.F., 2002. The role of the Early Tertiary Ulukışla Basin, southern Turkey, in suturing of the Mesozoic Tethys ocean. J. Geol. Soc. Lond. 159, 673–690.

Clark, M., Robertson, A.H.F., 2005. Uppermost Cretaceous-Lower Tertiary Ulukışla Basin, south-central Turkey: sedimentary evolution of part of a unified basin complex within an evolving Neotethyan suture zone. Sediment. Geol. 173, 15–51.

Cox, K.G., Bell, J.D., Pankhurst, R.J., 1979. The Interpretation of Igneous Rocks. George Allen and Unwin, London.

Demir, T., Seyrek, A., Guillou, H., Scaillet, S., Westaway, R., Bridgland, D., 2009. Preservation by basalt of a staircase of latest Pliocene terraces of the River Murat in eastern Turkey: evidence for rapid uplift of the eastern Anatolian Plateau. Glob. Planet. Chang. 68, 254–269.

Demirtaşlı, E., Turhan, N., Bilgin, A.Z., Selim, M., 1984. Geology of the Bolkar Mountains. In: Tekeli, O., Göncüoğlu, M.C. (Eds.), Geology of the Taurus Belt. Proceedings of the International Symposium on the Geology of the Taurus Belt, Ankara, Turkey. Mineral Resources and Exploration Institute of Turkey, pp. 121–141.

Dilek, Y., Furnes, H., 2009. Structure and geochemistry of Tethyan ophiolites and their petrogenesis in subduction rollback systems. Lithos 113, 1–20.

Duman, T.Y., Emre, Ö., 2013. The East Anatolian Fault: geometry, segmentation and jog characteristics. In: Robertson, A.H.F., Parlak, O., Ünlügenç, U.C. (Eds.), Geological development of Anatolia and the Easternmost Mediterranean Region. Geological Society, London, Special Publications, pp. 495–530.

Ekici, T., Alpaslan, M., Parlak, O., Uçurum, A., 2009. Geochemistry of the Middle Miocene collision-related Yamadağı (Eastern Anatolia) calc-alkaline volcanics, Turkey. Turk. J. Earth Sci. 18, 511–528.

Filbrandt, S.C., Nolan, S.C., Ries, A.C., 1990. Late Cretaceous and early Tertiary evolution of the Jebel Ja'alan and adjacent areas, NE Oman. In: Robertson, A.H.F., Searle, M.P., Ries, S.C. (Eds.), The Geology and Tectonics of the Oman Region. Geological Society, London, Special Publication, 49, pp. 697–714.

Fitton, J.G., Saunders, A.D., Larsen, L.M., Hardarson, B.S., Norry, M.J., 1998. Volcanic rocks from the southeast Greenland margin at 630 N: composition, petrogenesis and mantle sources. In: Saunders, A.D., Larsen, H.C., Wise Jr., S.W. (Eds.), Proceedings of the Ocean Drilling Program, Scientific Results, 152. Ocean Drilling Program, TX, pp. 331–350.

Floyd, P.A., Kelling, G., Gökçen, S.L., Gökçen, N., 1991. Geochemistry and tectonic environment of basaltic rocks from the Misis ophiolitic melange, south Turkey. Chem. Geol. 89, 263–280.

Floyd, P.A., Göncüoğlu, M.C., Winchester, J.A., Yaliniz, M.K., 2000. Geochemical Character and Tectonic Environment of Neotethyan Ophiolitic Fragments and Metabasites in the Central Anatolian Crystalline Complex, Turkey. In: Bozkurt, E., Winchester, J.A., Piper, J.D.A. (Eds.), Tectonics and Magmatism in Turkey and the Surrounding Area. Geological Society, London, Special Publications, 173, pp. 183–202.

Glennie, K.W., Hughes-Clarke, M.W., Boeuf, W.G.A., Pilaar, W.F.H., Reinhardt, B.M., 1990. Inter-relationship of Makran-Oman Mountains belts of convergence. In: Robertson, A.H.F., Searle, M.P., Ries, A.C. (Eds.), The Geology and Tectonics of the Oman Region. Geological Society, London, Special Publications, 49, pp. 773–786.

Göncüoğlu, M.C., Dirik, K., Kozlu, H., 1996–1997. Pre-alpine and alpine terranes in Turkey: explanatory notes to the terrane map of Turkey. Annalles Géologiques des Pays Héllenique 37, 1–3.

Görür, N., Tüysüz, O., 2001. Cretaceous to Miocene palaeogeographic evolution of Turkey: implications for hydrocarbon potential. J. Pet. Geol. 24, 119–146.

Görür, N., Oktay, F.Y., Seymen, I., Şengör, A.M.C., 1984. Palaeotectonic evolution of the Tuzgölü basin complex, Central Turkey: sedimentary record of a Neo-Tethyan closure. In: Dixon, J.E., Robertson, A.H.F. (Eds.), The Geological Evolution of the Eastern Mediterranean. The Geological Society, London, Special Publications, 17, pp. 467–482.

Görür, N., Tüysüz, O., Şengör, A.M.C., 1998. Tectonic evolution of the Central Anatolian basins. Int. Geol. Rev. 9, 832–850.

Gradstein, F.M., Ogg, J.G., Smith, A.G., Al, E., 2004. A Geologic Time Scale. Cambridge University Press, Cambridge.

Guezou, J.-C., Temiz, H., Poisson, A., Gürsoy, H., 1996. Tectonics of the Sivas Basin: the Neogene record of the Anatolian accretion along the inner tauric suture. Int. Geol. Rev. 38, 901–925.

Gunatilaka, A., Mwango, S., 1987. Continental sabkhas pans and associated nebkhas in southern Kuwait, Arabian Gulf. In: Frostick, L.E., Ried, I. (Eds.), Desert Sediments: Ancient and Modern. Geological Society of London, Special Publication, 35, pp. 187–203.

Gürbüz, K., Gül, M., 2005. Evolution of and factors controlling Eocene Sedimentation in the Darende-Balaban Basin, Malatya (Eastern Turkey). Turk. J. Earth Sci. 14, 311–335.

Gürer, Ö.F., 1994. Upper Cretaceous stratigraphy of Hekimhan–Hasançelebi region and the basin evolution. Geol. Bull. Turkey 37, 135–148.

Gürer, Ö.F., 1996. Geological position and the genesis of Hasançelebi alkaline magmatism at [sic] the Eastern Taurides (NW Malatya). Turk. J. Earth Sci. 5, 71–88.

Gürer, Ö.F., Aldanmaz, E., 2002. Origin of the Upper Cretaceous–Tertiary sedimentary basins within the Tauride–Anatolide platform in Turkey. Geol. Mag. 139, 191–197.

Gürsoy, H., Tatar, O., Piper, J.D.A., Koçbulut, F., Akpınar, Z., Huang, B., Roberts, A.P., Mesci, B.L., 2011. Palaeomagnetic study of the Kepezdağ and Yamadağ volcanic complexes, central Turkey: Neogene tectonic escape and block definition in the central-east Anatolides. J. Geodyn. 51, 308–326.

Karaoğlan, F., Parlak, O., Robertson, A.H.F., Thöni, M., Klötzli, U., Koller, F., Okay, A.İ., 2013. Eocene HT/HP metamorphism of ophiolitic rocks and Eocene crosscutting granitoid intrusions (Doğanşehir area, SE Anatolia) related to late-stage Neotethyan subduction processes. In: Robertson, A.H.F., Parlak, O., Ünlügenç, U.C. (Eds.), Geological Development of Anatolia and the Easternmost Mediterranean Region. Geological Society of London, Special Publication, 372, pp. 249–272.

Karig, D.E., Ingle Jr., J.C., Bouma, A.H., 1975. Initial Reports of the Deep Sea Drilling Project 31. U.S. Government Printing Office, Washington, DC.
Kavak, K., Poisson, A., Guezou, J., 1997. Tectonostratigraphy of the Southern Sivas Tertiary Basin (Central Turkey) and comparison with Landsat MSS Imagery. Int. Geol. Rev. 39, 353–364.
Keskin, M., Pearce, J.A., Mitchell, J.G., 1998. Volcano-stratigraphy and geochemistry of collision-related volcanism on the Erzurum-Kars Plateau, northeastern Turkey. J. Volcanol. Geotherm. Res. 85, 355–404.
Keskin, M., Genç, Ş.C., Tüysüz, O., 2008. Petrology and geochemistry of post-collisional Middle Eocene volcanic units in North-Central Turkey: evidence for magma generation by slab break off following the closure of the Northern Neotethys Ocean. Lithos 104, 267–305.
Koçyiğit, A., 1991. An example of an accretionary forearc basin from northern central Anatolia and its implications for the history of subduction of Neo-Tethys in Turkey. Geol. Soc. Am. Bull. 103, 22–36.
Kürüm, S., Önal, A., Boztuğ, D., Spell, T., Arslan, M., 2008. 40Ar/39Ar age and geochemistry of the post-collisional Miocene Yamadağ volcanics in the Arapkir area (Malatya Province), eastern Anatolia, Turkey. J. Asian Earth Sci. 33, 229–251.
Kuşcu, I., Yılmazer, E., Demirela, G., Güleç, N., Kuşcu, G., Kaymakcı, N., Gökçe, H., Şalıs, B., Marschik, R., 2007. Hasançelebi-Hekimhan (Malatya) Bölgeleri emiroksit Yataklarının Demir Oksit-Bakır-Altın (DOBA) Yatakları Açısından I · ncelenmesi ve Bakır-Altın Potansiyellerinin Aras,tırılması: TÜBI·TAK Project-ÇAYDAG 103Y023. p. 190 ([in Turkish with English abstract]).
Kuşcu, I., Kuşcu, G.G., Tosdal, R.M., Ulrich, T.D., Friedman, R., 2010. Magmatism in the southeastern Anatolian orogenic belt: transition from arc to post-collisional setting in an evolving orogen. In: Sosson, M., Kaymakcı, N., Stephenson, R.A., Bergerat, F., Starostenko, V. (Eds.), Sedimentary Basin Tectonics from the Black Sea and Caucasus to the Arabian Platform. Geological Society, London, Special Publications, 340, pp. 437–460.
Kuşcu, İ., Yılmazer, E., Güleç, N., Bayır, S., Demırela, G., Kuşcu, G.G., Kuru, G.S., Kaymakşı, N., 2011. U-Pb and 40Ar-39Ar Geochronology and isotopic constraints on the genesis of copper-gold-bearing iron oxide deposits in the Hasançelebi district, Eastern Turkey. Econ. Geol. 106, 261–288.
Le Maitre, R.W., Bateman, P., Dudek, A., Keller, J., Le Bas, M.J., Sabine, P.A., Schmid, R., Sorensen, H., Streckeisen, A., Woolley, A.R., Zanettin, B., 1989. A Classification of Igneous Rocks and Glossary of Terms. Blackwell, Oxford.
Le Maitre, R.W., Streckeisen, A., Zanettin, B., Le Bas, M.J., Bonin, B., Bateman, P., Bellieni, G., Dudek, A., Efremova, S., Keller, J., Lamere, J., Sabine, P.A., Schmid, R., Sorensen, H., Wooley, A.R., 2002. Igneous Rocks: A Classification and Glossary of Terms, Recommendations of the International Union of Geological Sciences. Subcommission of the Systematics of Igneous RocksCambridge University Press.
Leo, G.W., Marvin, R.F., Mehnert, H.H., 1974. Geologic framework of the Kuluncak–Sofular area, East-Central Turkey, and K–Ar ages of igneous rocks. Geol. Soc. Am. Bull. 85, 1785–1788.
Mackintosh, P.W., Robertson, A.H.F., 2013. Sedimentary and structural evidence for a two-phase Upper Cretaceous and Paleogene emplacement of the Tauride thrust sheets in central southern Turkey. In: Robertson, A.H.F., Parlak, O., Ünlügenç, U.C. (Eds.), Geological development of Anatolia and the Easternmost Mediterranean Region. Geological Society, London, Special Publication, 372, pp. 299–322.
Marschik, T., Spikings, R., Kuşcu, İ., 2008. Geochronology and stable isotope signature of alteration related to hydrothermal magnetite ores in Central Anatolia, Turkey. Mineral. Deposita 43, 111–124.
Matthai, G., 1948. On the mode of growth of the skeleton in fungid corals. Philos. Trans. R. Soc. Lond. 233, 177–195.
McLennan, S.M., Ross Taylor, S., Hemming, S.R., 2006. Composition, differentiation, and evolution of continental crust: constraints from sedimentary rocks and heat flow. In: Brown, M., Rushmer, T. (Eds.), Evolution and differentiation of the continental crust. Cambridge University Press, pp. 92–134.
Miller, K.G., Kominz, M.A., Browning, J.V., Wright, J.D., Mountain, G.S., Katz, M.E., Miller, K.G., Kominz, M.A., Browning, J.V., Wright, J.D., Mountain, G.S., Katz, M.E., Sugarman, P.J., Cramer, B.S., Christie-Blick, N., Pekar, S.F., 2005. The Phanerozoic Record of Global Sea-Level Change. Science 25, 1293–1298.
MTA 2002. Geological Map of Turkey, 1:500.000, Maden Tektik ve Arama Genel Müdürlüğü. Ankara: General Directorate of Mineral Research and Exploration.
Nairn, S.P., Robertson, A.H.F., Ünlügenç, U.C., İnan, N., Taslı, K., 2013. Tectonostratigraphic evolution of the Upper Cretaceous-Cenozoic central Anatolian basins: an integrated model of diachronous ocean basin closure and continental collision. In: Robertson, A.H.F., Parlak, O., Ünlügenç, U.C. (Eds.), Geological development of Anatolia and the Easternmost Mediterranean Region. Geological Society, London, Special, Publication, 372, pp. 343–384.
Oberhänsli, R., Candan, O., Bousquet, R., Rimmele, G., Okay, A.I., Goff, J., 2010. Alpine HP Evolution of the eastern Bitlis complex, SE Turkey. In: Sosson, M., Kaymakci, N., Stephenson, R., Strarostenko, V., Bergerat, F. (Eds.), Sedimentary Basin, Tectonics from the Black Sea an Caucasus to the Arabian Platform. Geological Society, London, Special Publications, 340, pp. 461–483.
Oberhänsli, R., Koralay, E., Candan, O., Pourteau, A., Bousquet, R., 2014. Late Cretaceous eclogitic high-pressure relics in the Bitlis Massif. Geodin. Acta. http://dx.doi.org/10.1080/09853111.2013.858951.
Odin, G.S., 1988. Green marine clays. Developments in Sedimentology, 45. Elsevier, Amsterdam.
Okay, A.I., Şahintürk, Ö., 1997. Geology of the Eastern Pontides. In: Robinson, A.G. (Ed.), Regional and Petroleum Geology of the Black Sea and Surrounding Region. American Association of Petroleum Geologists Memoir, 68, pp. 291–311.
Okay, A.I., Tüysüz, O., 1999. Tethyan sutures of Northern Turkey. In: Durand, B., Jolivet, L., Horvárth, F., Séranne, M. (Eds.), The Mediterranean Basins: Tertiary Extension within the Alpine Orogen. Geological Society, London, Special Publications, 156, pp. 475–515.
Okay, A.İ., Satır, I., Siebel, W., 2006. Pre-Alpide Palaeozoic and Mesozoic orogenic events in Turkey. In: Gee, D.G., Stepherson, R.A. (Eds.), European Lithosphere Dynamics. Geological Society, London, Memoirs, 32, pp. 355–388.
Okay, A.İ., Zattin, M., Cavazza, W., 2010. Apatite fission-track data for the Miocene Arabia-Eurasia collision. Geology 38, 35–38.
Özdemir, Z., Tunç, M., 1993. Palaeontologic and stratigraphic features of Upper Cretaceous units in the vicinity of Hekimhan (Malatya). Geol. Bull. Turkey 36, 131–144 ([in Turkish with English abstract]).
Özer, S., 2010. Campanian–Maastrichtian Psuedosabinia from Turkey: descriptions and Taxonomic problems. Turk. J. Earth Sci. 19, 643–669.
Özgenç, I., İlbeyli, N., 2009. Geochemical constraints on petrogenesis of Late Cretaceous alkaline magmatism in east-central Anatolia (Hasançelebi-Basören, Malatya), Turkey. Mineral. Petrol. 95, 71–85.
Özgül, N., 1997. Stratigraphy of the tectono-stratigraphic units in the region Bozkır-Hadim-Taşkent (northern central Taurides). Maden Tetkik ve Arama Bulletin 119, 113–174 ([in Turkish]).
Palmer, M.R., Helvací, C., Fallick, A.E., 2004. Sulphur, sulphate oxygen and strontium, isotope composition of Cenozoic Turkish evaporates. Chem. Geol. 209, 341–356.
Parlak, O., Höck, V., Kozlu, H., Delaloye, M., 2004. Oceanic crust generation in an island arc tectonic setting, SE Anatolian orogenic belt (Turkey). Geol. Mag. 141, 583–603.
Parlak, O., Rızaoğlu, T., Bağcı, U., Karaoğlan, F., Höck, V., 2009. Tectonic significance of the geochemistry and petrology of ophiolites in southeast Anatolia, Turkey. Tectonophysics 473, 173–187.
Parlak, O., Karaoglan, F., Rizaoglu, T., Nurlu, N., Bagci, U., Höck, V., Önal, A., Kürüm, S., Topak, Y., 2012. Petrology of the İspendere (Malatya) ophiolite from the Southeast Anatolia: implications for the Late Mesozoic evolution of the southern Neotethyan ocean. In: Robertson, A.H.F., Parlak, O., Ünlügenç, U. (Eds.), Geological Development of the Anatolian Continent and the Easternmost Mediterranean Region. Geological Society, London, Special Publications, 372, pp. 219–247.
Parlak, O., Çolakoğlu, A., Dönmez, C., Sayak, H., Yildirim, N., Türkel, A., Odabaşi, İ., 2013a. Geochemistry and tectonic significance of ophiolites along the İzmir–Ankara–Erzincan Suture Zone in northeastern Anatolia. In: Robertson, A.H.F., Parlak, O., Ünlügenç, U.C. (Eds.), Geological development of Anatolia and the Easternmost Mediterranean Region. Geological Society, London, Special, Publication, 372, pp. 75–105.
Parlak, O., Karaoğlan, F., Rızaoğlu, T., Klötzli, U., Koller, F., Bıllor, Z., 2013b. U-Pb and ^{40}Ar-^{39}Ar geochronology of the ophiolites and granitoids from the Tauride belt: implications for the evolution of the Inner Tauride suture. J. Geophys. 65, 22–37.
Pearce, J.A., 1982. Trace element characteristics of lavas from destructive plate boundaries. In: Thorpe, R.S. (Ed.), Andesites. Wiley, Chichester, pp. 525–548.
Pearce, J.A., Cann, J.R., 1973. Tectonic setting of basic volcanic rocks determined using trace element analysis. Earth Planet. Sci. Lett. 19, 290–300.
Pearce, J.A., Bender, J.F., De Long, S.E., Kidd, W.S.F., Low, P.J., Güner, Y., Saroglu, F., Yilmaz, Y., Moorbath, S., Mitchell, J.G., 1990. Genesis of collision volcanism in Eastern Anatolia, Turkey. J. Volcanol. Geotherm. Res. 44, 189–229.
Perinçek, D., Kozlu, H., 1984. Stratigraphy and structural relations of the units in the Afşin-Elbistan-Doğanşehir region (Eastern Taurus). In: Tekeli, O., Göncüoğlu, M.C. (Eds.), Geology of the Taurus Belt. Proceedings of the International Symposium on the Geology of the Taurus Belt. MTA, Turkey, pp. 182–198.
Poisson, J.-C., Guezou, A., Ozturk, S., Inan, H., Temiz, H., Gürsöy, K.S., Kavak, S., Özden, S., 1996. Tectonic setting and evolution of the Sivas Basin, Central Anatolia, Turkey. Int. Geol. Rev. 38, 838–853.
Pourteau, A., Candan, O., Oberhänsli, R., 2010. High-pressure metasediments in central Turkey: constraints on the Neotethyan closure history. Tectonics 29, TC5004.
Robertson, A.H.F., 2002. Overview of the genesis and emplacement of Mesozoic ophiolites in the Eastern Mediterranean Tethyan region. Lithos 65, 1–67.
Robertson, A.H.F., 2004. Development of concepts concerning the genesis and emplacement of Tethyan ophiolites in the Eastern Mediterranean and Oman regions. Earth Sci. Rev. 66, 331–387.
Robertson, A.H.F., 2006. Contrasting modes of ophiolite emplacement in the Eastern Mediterranean region. In: Gee, D.G., Stephenson, R.A. (Eds.), European Lithosphere Dynamics. Geological Society, London, Memoirs, 32, pp. 235–261.
Robertson, A.H.F., Boyle, J.F., 1983. Tectonic setting and origin of metalliferous sediments in the Mesozoic Tethys Ocean. In: Rona, P.A., Bostrom, K., Laubier, L., Smith Jr., K.L. (Eds.), Hydrothermal Processes of Seafloor Spreading Centres. Plenum, New York, pp. 595–663.
Robertson, A.H.F., Searle, M.P., 1990. The northern Oman Tethyan continental margin: stratigraphy, structure, concepts and controversies. In: Robertson, A.H.F., Searle, M.P., Ries, A.C. (Eds.), The Geology and Tectonics of the Oman Region. Geological Society, London, Special Publication, 49, pp. 3–25.
Robertson, A.H.F., Sharp, T.R., 2002. Geochemical and mineralogical evidence for the provenance of mixed volcanogenic/terrigenous hemipelagic sediments in the Pliocene-Pleistocene Woodlark backarc rift basin, Southwest Pacific: Ocean Drilling Program Leg 180. Proc. Ocean Drill. Program Sci. Results 80, 1–53.
Robertson, A.H.F., Dixon, J.E., Brown, S., Collins, A., Morris, A., Pickett, E., Sharp, I., Ustaömer, T., 1996. Alternative tectonic models for the Late Palaeozoic-Early Tertiary development of Tethys in the Eastern Mediterranean region. In: Morris, A., Tarling, D.H. (Eds.), Palaeomagnetism and Tectonics of the Mediterranean Region. Geological Society Special Publication, 105, pp. 239–263.
Robertson, A.H.F., Ustaömer, T., Parlak, O., Ünlügenç, U.C., Taşli, K., İnan, N., 2006. The Berit transect of the Tauride thrust belt, S Turkey: Late Cretaceous–Early Cenozoic accretionary/collisional processes related to closure of the Southern Neotethys. J. Asian Earth Sci. 27, 108–145.
Robertson, A.H.F., Parlak, O., Rızaoğlu, T., Ünlügenç, U., İnan, N., Taslı, K., Ustaömer, T., 2007. Tectonic evolution of the South Tethyan ocean: evidence from the Eastern Taurus Mountains (Elazığ region, SE Turkey). In: Ries, A.C., Butler, R.W.H., Graham, R.H. (Eds.), Deformation of the Continental Crust: The Legacy of Mike Coward. Geological Society, London, Special Publications, 272, pp. 231–270.

Robertson, A.H.F., Parlak, O., Ustaömer, T., 2009. Melange genesis and ophiolite emplacement related to subduction of the northern margin of the Tauride Anatolide continent, central and eastern Turkey. In: Van Hinsbergen, D.J.J., Edwards, M.A., Govers, R. (Eds.), Collision and Collapse at the Africa-Arabia-Eurasia Subduction Zone. Geological Society, London, Special Publications, 311, pp. 9–66.

Robertson, A.H.F., Parlak, O., Ustaömer, T., 2012. Overview of the Palaeozoic–Neogene evolution of Neotethys in the Eastern Mediterranean region (southern Turkey, Cyprus, Syria). Pet. Geosci. 18, 381–404.

Robertson, A.H.F., Parlak, O., Ustaömer, T., 2013a. Late Palaeozoic-Early Cenozoic tectonic development of Southern Turkey and the easternmost Mediterranean region: evidence from the inter-relations of continental and oceanic units. In: Robertson, A.H.F., Parlak, O., Ünlügenç, U.C. (Eds.), Geological development of Anatolia and the Easternmost Mediterranean Region. Geological Society, London, Special Publications, 372, pp. 9–48.

Robertson, A.H.F., Parlak, O., Metin, Y., Vergili, O., Tasli, K., Inan, N., Soycan, H., 2013b. Late Palaeozoic-Cenozoic tectonic development of carbonate platform, margin and oceanic units in the Eastern Taurides, Turkey. In: Robertson, A.H.F., Parlak, O., Ünlügenç, U.C. (Eds.), Geological development of Anatolia and the Easternmost Mediterranean Region. Geological Society, London, Special Publication, 372, pp. 167–218.

Robertson, A.H.F., Trivić, B., Đerić, N., Bucur, I.I., 2013c. Tectonic development of the Vardar ocean and its margins: evidence from the Republic of Macedonia and Greek Macedonia. Tectonophysics 595–596, 25–54.

Robertson, A.H.F., Parlak, O., Ustaömer, T., Taslı İnan İ, Dumitrica, P., Karaoğlan, F., 2014. Subduction, ophiolite genesis and collision history of Tethys adjacent to the Eurasian continental margin: new evidence from the Eastern Pontides. Turkey Geodinamica Acta.

Saunders, A.D., Tarney, J., 1984. Geochemical characteristics of basaltic volcanism within back-arc basins. In: Kokelaar, B.P., Howells, M.F. (Eds.), Marginal Basin Geology: Volcanic and Associated Sedimentary and Tectonic Processes in Modern and Ancient Marginal Basins. Geological Society, London, Special Publications, 16, pp. 59–76.

Schildgen, T.F., Cosentino, D., Bookhagen, B., Niedermann, S., Yıldırım, C., Echtler, H., Wittmann, H., Strecker, M.R., 2012. Multi-phased uplift of the southern margin of the Central Anatolian plateau, Turkey: a record of tectonic and upper mantle processes. Earth Planet. Sci. Lett. 317–318, 85–95.

Şengör, A.M.C., Yılmaz, Y., 1981. Tethyan evolution of Turkey: a plate tectonic approach. Tectonophysics 75, 81–241.

Shelton, A.W., 1990. The interpretation of gravity data in Oman: constraints on the ophiolite emplacement mechanism. In: Robertson, A.H.F., Searle, M.P., Ries, A.C. (Eds.), The Geology and Tectonics of the Oman Region. The Geological Society, London, Special Publications, 49, pp. 459–471.

Sosson, M., Rolland, Y., Danelian, T., Muller, C., Melkonyan, R., Adamia, S., Kangarli, T., Avagyan, A., Galoyan, G.H., 2010. Subductions, obduction and collision in the Lesser Caucasus (Armenia, Azerbaijan, Georgia), new insights. In: Sosson, M., Kaymakci, N., Stephanson, R., Bergarat, F., Storatchenoko, V. (Eds.), Sedimentary basin tectonics from the Black Sea and Caucasus to the Arabian Platform. London: Geological Society, Special Publications, 340, pp. 329–352.

Stendal, H., Ünlü, T., Konnerup-Madsen, J., 1995. Geological setting of iron deposits of Hekimhan province, Malatya, Central Anatolia, Turkey. Trans. Inst. Min. Mineralisation Clays, Min. 104, 46–54.

Steuber, T., Löser, H., 2000. Species richness and abundance patterns of Tethyan Cretaceous rudist bivalves (Mollusca: Hippuritacea) in the central-eastern Mediterranean and Middle East, analysed from a palaeontological database. Palaeogeogr. Palaeoclimatol. Palaeoecol. 162, 75–104.

Taslı, K., Özer, E., Koç, H., 2006. Benthic foraminiferal assemblages of the Cretaceous platform carbonate succession in the Yavca area (Bolkar Mountains, S Turkey): biostratigraphy and palaeoenvironments. Geobios 39, 521–533.

Taylor, B., 1992. Rifting and the volcanic-tectonic evolution of the Izu-Bonin-Mariana arc. In: Taylor, B., Fujioka, K., et al. (Eds.), Proceedings of the Ocean Drilling Program, Scientific Results, 126. Ocean Drilling Program, College Station, TX, pp. 627–651.

Turekian, K.K., Wedepohl, K.H., 1961. Distribution of the elements in some major units of the Earth's crust. Geol. Soc. Am. Bull. 72, 175–192.

Uçurum, A., Larson, L.T., Boztuğ, D., 1996. Geology, geochemistry and petrology of the alkaline subvolcanic trachyte-hosted iron deposit in the Karakuz area, northwestern Hekimhan–Malatya, Turkey. Int. Geol. Rev. 38, 995–1005.

Wilson, M., 1989. Igneous Petrogenesis. Unwin Hyman, London.

H.Yalçın, H., Ö.Bozkaya, Ö., 1995. Sepiolite-palygorskite from the Hekimhan region (Turkey)Clays Miner. 43, 705–717.

Yalçın, H., Bozkaya, Ö., 1996. A new discovery of the Cretaceous/Tertiary boundary from the Tethyan Belt, Hekimhan Basin, Turkey: mineralogical and geochemical evidence. Int. Geol. Rev. 38, 759–767.

Yalçın, H., Bozkaya, Ö., Hozatlıoğlu, D., 2009. Cretaceous serpentinite-hosted phlogopite occurrences in Malatya-Kuluncak area, Turkey. Proceedings of 14th National Clay Symposium (Turkey), pp. 174–192.

Yazgan, E., Chessex, R., 1991. Geology and tectonic evolution of the southeastern Taurides in the region of Malatya. Turk. Assoc. Pet. Geol. Bull. 3, 11–42.

Yiğitbaş, E., Yılmaz, Y., 1996. New evidence and solution to the Maden complex controversy of the Southeast Anatolian orogenic belt (Turkey). Geol. Rundsch. 85, 250–263.

Yılmaz, Y., 1993. New evidence and model on the evolution of the southeast Anatolian orogen. Geol. Soc. Am. Bull. 105, 251–271.

Yılmaz, A., Yılmaz, H., 2004. Geology and structural evolution of the Divriği-Sivas region. Geol. Bull. Turkey 47, 14–15.

Yılmaz, A., Yılmaz, H., 2006. Characteristic features and structural evolution of a post-collisional basin: the Sivas Basin, Central Anatolia, Turkey. J. Asian Earth Sci. 27, 16.

Yılmaz, S., Boztu, D., Öztürk, A., 1993. Geological setting, petrographic and geochemical characteristics of the Cretaceous and Tertiary igneous rocks in the Hekimhan–Hasançelebi area, northwest Malatya, Turkey. Geol. J. 28, 383–398.

Zorlu, K., Inan, S., Gül, M., Inan, N., Kurt, M.A., Alpaslan, M., 2011. Geological evolution of the Ülükışla Basin (Late Cretaceous–Eocene) Central Anatolia, Turkey. Bull. Earth Sci. Appl. Res. Centre of Hacettepe University 32, 151–170.